Journal of Engineering Mathematics **31:** 173–203, 1997.

A deflagration analysis of porous energetic materials with two-phase flow and a multiphase sequential reaction mechanism

STEPHEN B. MARGOLIS
Combustion Research Facility, Sandia National Laboratories, Livermore, California 94551-0969, U.S.A.

Received: 31 January 1996; accepted in revised form 22 October 1996

Abstract. A theoretical analysis for the unconfined deflagration of a porous energetic material is developed for a two-step global reaction mechanism that consists of the condensed-phase combustion of the reactive material to produce gas-phase intermediates, followed by a gas-phase reaction that produces final gas-phase products. An asymptotic approach is employed, leading to explicit formulas for the deflagration velocity in specific parameter regimes. The results clearly indicate the influences of two-phase flow and the multiphase, multi-step chemistry on the burning rate, and serve to further characterize the combustion behavior of a significant class of degraded nitramine-type propellants for which the present analysis is applicable.

Key words: deflagration, two-phase flow, porous materials, activation energy, asymptotics

1. Introduction

The combustion behavior of porous energetic materials such as solid propellants is a subject of increasing interest in the fields of propulsion and pyrotechnics. This interest is motivated, at least in part, by uncertainties with respect to both performance and safety when an energetic material has either been in existence for an extended period of time and/or has been exposed to an abnormal thermal environment at some point in its history. In such a situation, there is likely to be some degree of degradation in the chemical composition of the material, resulting in a much higher porosity than that of the original pristine material, with the voids being filled with intermediate gas-phase decomposition products. Thus, it is becoming increasingly clear that, during combustion, two-phase-flow effects play an important role, both within the degraded solid, as well as within a thin multiphase layer at the surface where finite-rate exothermic reactions occur. As a result, the deflagration characteristics of such 'damaged' materials, with porosities as high as order unity, may differ significantly from those of the pristine material due, at least in part, to greatly enhanced gas flow in the solid/gas preheat region. The presence of gas in the porous solid in turn results in a more pronounced two-phase effect in the multiphase surface layer, as, for example, in the commonly observed liquid melt region of nitramine propellants, which are often characterized by extensive bubbling in an exothermic foam layer. Indeed, the present analysis, along with several other recent studies described below, is largely applicable to this latter class of propellants.

Despite difficulties inherent in describing phenomena associated with two-phase flow, there have by now been a number of relatively complete formulations employing various types of constitutive relations, which are generally required to close the governing system of equations ([1]). The process of analyzing such models presents significant challenges, not only because of the variety of physical phenomena associated with such problems, but also from the greater degree of nonlinearity that arises from the appearance of appropriate volume-fraction variables that multiply each quantity associated with a particular phase. Although early two-phase work

in this area tended to circumvent some of the difficulties by treating the two-phase medium as a single phase with suitably 'averaged' properties ([2], [3]), the resulting models required the velocity (and temperature) of each phase to be the same, precluding many of the predominant effects associated with combustion processes that involve two-phase flow. Indeed, some of these concerns have recently been addressed in several recent papers ([4], [5], [6], [7], [8], [9]). To be able to focus clearly on the effects of two-phase flow, the description of the chemistry was deliberately simplified. In particular, a one-step overall exothermic process, $R(c) \rightarrow P(g)$, representing the direct conversion of the condensed (liquid) propellant to gaseous products, was generally considered in the latter group of studies. However, in one of these studies, [5], a somewhat more elaborate mechanism, motivated by knowledge of nitramine chemistry and given by $R(c) \rightarrow P(g), R(c) \leftrightarrow R(g), R(g) \rightarrow P(g)$, was adopted, where $R(g)$ is a gaseous reactant. In each of these studies, the goal was to clarify certain fundamental two-phase effects on steady, planar deflagrations and their stability. These effects specifically included those associated with different velocities and, in several instances, temperatures for each phase.

The motivation for the present work is to extend these previous studies by incorporating both condensed- and gas-phase reactions in the thin reaction region previously represented by the simple one-step mechanism $R(c) \rightarrow P(g)$. The model and analysis differ from those in [5], however, in that we consider a regime in which both types of reactions occur in the same thin multiphase region, as opposed to considering a separated regime in which the gas-phase reaction occurs downstream of the condensed-phase decomposition. In particular, we consider a two-step process in which the first step consists of an overall condensed-phase reaction that produces gas-phase intermediates, and the second step consists of the global reaction of these gas-phase intermediates to produce final gas-phase products. This simple mechanism, of course, is still an extreme approximation to the actual chemistry that transpires during nitramine deflagration ([10], [11]), but as with the single-step studies referenced above, our goal remains centered on assessing the role of two-phase flow on the structure and propagation of the combustion wave. In a sense, the present study is thus a multiphase analog to other single-phase analyses of combustion waves in gases and solids that are governed by a sequential reaction mechanism ([12], [13], [14], [15]).

2. The mathematical model

The physical problem of interest in the present study is described as follows. We consider an unconfined environment in which the unburned and degraded porous solid lies generally to the left, and the burned gas products lie to the right. Gas-phase intermediates are assumed to be produced directly by condensed-phase reactions, and these, in turn, can react to form the final combustion products according to

$$R(c) \rightarrow I(g), \qquad I(g) \rightarrow P(g), \tag{1}$$

where $R(c)$ denotes the condensed (melted) reactant material, $I(g)$ stands for the intermediate gas-phase species, and $P(g)$ represents the final gas-phase products (Figure 1). The nonzero porosity of the condensed material, which is an essential feature of the present analysis, is likely to arise not by design, but through slow degradation of the original pristine material, due either to some measure of metastability in the original material or to exposure to an abnormal thermal environment at some point in its history. As a result, the unburned solid is now said to

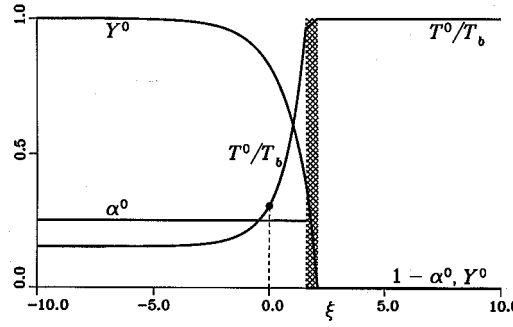

Figure 1. Outer structure of the leftward-propagating deflagration wave. The solid/gas region lies to the left of $\xi = 0$, and the liquid/gas region to the right. The shaded area denotes the region $\xi_r < \xi < \xi_r + H$, which, despite the explicit representation afforded by the outer delta-function formulation, actually lies within the inner reaction zone. The region to the right of the reaction zone consists of purely gaseous products. Parameter values used were $b = r = Le = l = 1, \hat{b} = \hat{r} = \hat{l} = 0{\cdot}8, \alpha_s = 0{\cdot}25, Q_l = 5, Q_g = H = 0{\cdot}5, \gamma_s = -0{\cdot}2, T_m = 2.$

be in a 'damaged' state, and consequently, the intermediate gas-phase species are assumed to fill the pores far upstream of the reaction. The present analysis considers the merged regime in which both reactions occur within a single reaction zone (necessary conditions for this to occur are given below), in contrast to a previous study [5] in which these reactions were spatially separated. Thus, the deflagration wave, which moves from right to left, consists of a solid/gas preheat region, the melting surface across which the condensed component of the two-phase mixture undergoes a phase change, a liquid/gas preheat region, a relatively thin (due to the realistic assumption of large activation energies) reaction zone in which all the condensed-phase material and gas-phase intermediates are converted to gaseous products according to (1), and finally, the burned region which, in reality, often corresponds to a dark zone that separates the primary flame region from a secondary gas flame downstream. Since the latter has relatively little influence across the dark zone on the primary reaction zone, it has correspondingly little effect on the burning velocity and can therefore be suppressed in the present type of deflagration analysis. In what follows, we will restrict attention to one spatial dimension ($\tilde{x}$), and use the subscripts s, l and g to denote solid, liquid and gas-phase quantities, respectively. The porous solid and intermediate gas-phase species thus extend to $\tilde{x} = -\infty$, where conditions are denoted by the subscript u, while the product gases extend to $\tilde{x} = +\infty$, where conditions are identified by the subscript b. The appearance of a tilde over a symbol (*e.g.*, $\tilde{x}$) will denote a dimensional quantity.

A reasonable model, appropriate for describing this type of multiphase deflagration wave, was derived previously for the simpler case of a single-step reaction mechanism $R(c) \rightarrow P(g)$ in which the condensed-phase reactant material was converted directly into gas-phase products, which were thus the only gas-phase species that existed in the model [7]. Here, however, we wish to describe, in addition to the two-phase-flow effects that were the focus of the previous work, the fundamental effects associated with separate condensed- and gas-phase reactions, and multiple gas-phase species. Thus, as before, the governing system of equations consists of conservation equations for mass, momentum and energy in the two-phase solid/gas and liquid/gas regions to the left and right of the melting surface $\tilde{x} = \tilde{x}_m$, but with an additional species conservation equation associated with the mass fraction of one of the two classes of gas-phase species (either intermediates or products). Denoting the gas-phase volume fraction by α, we may express continuity of each phase in the region $\tilde{x} > \tilde{x}_m$ separately for the liquid and gas phases as

$$\frac{\partial}{\partial \tilde{t}}[(1-\alpha)\tilde{\rho}_l] + \frac{\partial}{\partial \tilde{x}}[(1-\alpha)\tilde{\rho}_l \tilde{u}_l] = -\tilde{A}_l \tilde{\rho}_l (1-\alpha)\exp(-\tilde{E}_l/\tilde{R}^\circ \tilde{T}_l), \quad \tilde{x} > \tilde{x}_m, \tag{2}$$

$$\frac{\partial}{\partial \tilde{t}}(\alpha\tilde{\rho}_g) + \frac{\partial}{\partial \tilde{x}}(\alpha\tilde{\rho}_g\tilde{u}_g) = \tilde{A}_l \tilde{\rho}_l (1-\alpha)\exp(-\tilde{E}_l/\tilde{R}^\circ \tilde{T}_l), \quad \tilde{x} > \tilde{x}_m, \tag{3'}$$

where $\tilde{\rho}, \tilde{u}, \tilde{T}$ and $\tilde{t}$ denote density, velocity, temperature and time, respectively. In addition, we must also satisfy mass continuity of each gas-phase species. Denoting by Y and Y_p the mass fractions of the gas-phase intermediate and product species, respectively, we have by definition $Y_p = 1 - Y$, where the mass conservation equation for Y is given by

$$\begin{aligned}\frac{\partial}{\partial \tilde{t}}(\alpha\tilde{\rho}_g Y) + \frac{\partial}{\partial \tilde{x}}(\alpha\tilde{\rho}_g\tilde{u}_g Y) \;=\; & \frac{\partial}{\partial \tilde{x}}\left(\alpha\tilde{\rho}_g \tilde{D}\frac{\partial Y}{\partial \tilde{x}}\right) + \tilde{A}_l\tilde{\rho}_l(1-\alpha)\exp(-\tilde{E}_l/\tilde{R}^\circ\tilde{T}_l) \\ & -\tilde{A}_g(\alpha\tilde{\rho}_g Y)^n \exp(-\tilde{E}_g/\tilde{R}^\circ\tilde{T}_g), \quad \tilde{x} > \tilde{x}_m,\end{aligned} \tag{4'}$$

where $\tilde{A}_l, \tilde{A}_g$ and $\tilde{E}_l, \tilde{E}_g$ are the exponential reciprocal-time prefactors and the overall activation energies of the condensed (liquid) and gas-phase reactions, respectively; $\tilde{R}^\circ$ is the universal gas constant and n is the order of the gas-phase reaction. For simplicity, we will assume a constant value for $\tilde{\rho}_l$, but we do allow for variations in $\tilde{\rho}_g$. As in previous work ([4], [7]), the evaluation of the condensed-phase Arrhenius reaction rate is based on conditions (*e.g.*, temperature) in the liquid phase, and may be interpreted as a contribution to a constitutive relation for that medium. In a similar fashion, it is assumed here that the gas-phase reaction rate is based on local conditions in the gas. For additional simplicity, we shall take A_l and A_g to be constants, although for this type of global kinetic modeling, it may be reasonable to assign a pressure, as well as a temperature, dependency to these coefficients.

It is convenient to eliminate the liquid-phase reaction terms in $(3')$ and $(4')$ by summing each of these equations with (2) to obtain the overall liquid/gas continuity equation

$$\frac{\partial}{\partial \tilde{t}}[(1-\alpha)\tilde{\rho}_l + \alpha\tilde{\rho}_g] + \frac{\partial}{\partial \tilde{x}}[(1-\alpha)\tilde{\rho}_l\tilde{u}_l + \alpha\tilde{\rho}_g\tilde{u}_g] = 0, \quad \tilde{x} > \tilde{x}_m, \tag{3}$$

and

$$\begin{aligned}&\frac{\partial}{\partial \tilde{t}}[(1-\alpha)\tilde{\rho}_l + \alpha\tilde{\rho}_g Y] + \frac{\partial}{\partial \tilde{x}}[(1-\alpha)\tilde{\rho}_l\tilde{u}_l + \alpha\tilde{\rho}_g\tilde{u}_g Y] \\ &\quad = \frac{\partial}{\partial \tilde{x}}\left(\alpha\tilde{\rho}_g\tilde{D}\frac{\partial Y}{\partial \tilde{x}}\right) - \tilde{A}_g(\alpha\tilde{\rho}_g Y)^n \exp(-\tilde{E}_g/\tilde{R}^\circ\tilde{T}_g), \quad \tilde{x} > \tilde{x}_m.\end{aligned} \tag{4}$$

In the solid/gas region $\tilde{x} < \tilde{x}_m$, we assume for the solid phase a constant density $\tilde{\rho}_s$ and zero velocity ($\tilde{u}_s = 0$), with $\alpha \equiv \alpha_s$ also constant in this region. The gas-phase continuity equations for $\tilde{x} < \tilde{x}_m$ are thus independent of the solid phase and are given by

$$\frac{\partial}{\partial \tilde{t}}(\alpha_s\tilde{\rho}_g) + \frac{\partial}{\partial \tilde{x}}(\alpha_s\tilde{\rho}_g\tilde{u}_g) = 0, \quad \tilde{x} < \tilde{x}_m, \tag{5}$$

$$\frac{\partial}{\partial \tilde{t}}(\alpha_s\tilde{\rho}_g Y) + \frac{\partial}{\partial \tilde{x}}(\alpha_s\tilde{\rho}_g\tilde{u}_g Y) = \frac{\partial}{\partial \tilde{x}}\left(\alpha_s\tilde{\rho}_g\tilde{D}\frac{\partial Y}{\partial \tilde{x}}\right), \quad \tilde{x} < \tilde{x}_m, \tag{6}$$

where the first of these denotes overall gas-phase continuity and the second describes mass continuity of the intermediate gas-phase species. We observe that no reaction is assumed to occur in the solid phase and, owing to the assumption of large activation energies in the reaction-rate expressions (see below), the gas phase is reactionless as well in this region.

Conservation of energy for each phase in the liquid/gas region is given by

$$\frac{\partial}{\partial\tilde{t}}[\tilde{\rho}_l\tilde{c}_l(1-\alpha)\tilde{T}_l]+\frac{\partial}{\partial\tilde{x}}[\tilde{\rho}_l\tilde{c}_l\tilde{u}_l(1-\alpha)\tilde{T}_l]-\frac{\partial}{\partial\tilde{x}}\left[\tilde{\lambda}_l(1-\alpha)\frac{\partial\tilde{T}_l}{\partial\tilde{x}}\right]$$

$$=\tilde{Q}_l\tilde{A}_l\tilde{\rho}_l(1-\alpha)\exp(-\tilde{E}_l/\tilde{R}^\circ\tilde{T}_l)+\tilde{K}_{lg}(\tilde{T}_g-\tilde{T}_l),\quad \tilde{x}>\tilde{x}_m, \tag{7′}$$

$$\frac{\partial}{\partial\tilde{t}}(\tilde{\rho}_g\tilde{c}_g\alpha\tilde{T}_g)+\frac{\partial}{\partial\tilde{x}}(\tilde{\rho}_g\tilde{c}_g\tilde{u}_g\alpha\tilde{T}_g)-\frac{\partial}{\partial\tilde{x}}\left(\tilde{\lambda}_g\alpha\frac{\partial\tilde{T}_g}{\partial\tilde{x}}\right)$$

$$=\tilde{Q}_g\tilde{A}_g(\alpha\tilde{\rho}_gY)^n\exp(-\tilde{E}_g/\tilde{R}^\circ\tilde{T}_g)+\alpha\frac{\partial\tilde{p}_g}{\partial\tilde{t}}+\tilde{K}_{lg}(\tilde{T}_l-\tilde{T}_g),\quad \tilde{x}>\tilde{x}_m, \tag{8′}$$

where $\tilde{c},\tilde{\lambda}$ and $\tilde{p}$ denote heat capacity (at constant volume for the liquid, and at constant pressure for the gas, both assumed constant), thermal conductivity and pressure, respectively; $\tilde{Q}_l$ and $\tilde{Q}_g$ denote the heat release for the condensed and gas-phase reactions at temperatures $\tilde{T}_l$ and $\tilde{T}_g$, respectively, and $\tilde{K}_{lg}$ is an interphase heat-transfer coefficient (*cf.* [4]), where interphase heat transfer is assumed to be the dominant mode of thermal contact between phases. As is evident from the placement of the reaction-rate terms in $(7')$ and $(8')$, the heat released by the condensed-phase reaction, $\tilde{Q}_l$, is assumed to be deposited in the liquid, while the heat released by the gas-phase reaction, $\tilde{Q}_g$, is assumed to be deposited in the gas. These assignments represent constitutive types of assumptions that can be appropriately generalized, although in the single-temperature limit considered below, the model becomes independent of how the heat release is apportioned between the two phases. Replacing all l-subscripts with s-subscripts, the corresponding equations in the reactionless solid/gas region $\tilde{x}_3<\tilde{x}_m$ are essentially the same as $(7')$ and $(8')$, but without the reaction-rate terms and a different interphase heat-transfer coefficient $\tilde{K}_{sg}$. We note that, because of the small Mach number and the generally small ratio of gas-to-liquid densities in the problems to be considered, no terms involving the liquid pressure $\tilde{p}_l$ appear in $(7')$, and the gas pressure $\tilde{p}_g$ depends only on $\tilde{t}$ in $(8')$. We remark that the term involving $\partial\tilde{p}_g/\partial\tilde{t}$ originates from the contribution to the rate of change of the internal energy of the gas resulting from the sum of the rate of surface work $-\partial(\alpha\tilde{u}_g\tilde{p}_g)/\partial\tilde{x}$ and the rate of volume work $-\tilde{p}_g\partial\alpha/\partial\tilde{t}$ performed by the gas (see [7]).

It is again convenient to eliminate reaction-rate terms when possible, and consequently, we use $(3')$ and $(4')$ in $(7')$ and in the overall liquid/gas energy equation that is obtained from summing $(7')$ and $(8')$. Thus, in place of $(7')$ and $(8')$, we obtain the liquid and overall energy equations

$$\frac{\partial}{\partial\tilde{t}}[\tilde{\rho}_l(1-\alpha)(\tilde{Q}_l+\tilde{c}_l\tilde{T}_l)]+\frac{\partial}{\partial\tilde{x}}[\tilde{\rho}_l\tilde{u}_l(1-\alpha)(\tilde{Q}_l+\tilde{c}_l\tilde{T}_l)]-\frac{\partial}{\partial\tilde{x}}\left[\tilde{\lambda}_l(1-\alpha)\frac{\partial\tilde{T}_l}{\partial\tilde{x}}\right]$$

$$=\tilde{K}_{lg}(\tilde{T}_g-\tilde{T}_l),\quad \tilde{x}>\tilde{x}_m, \tag{7}$$

$$\frac{\partial}{\partial\tilde{t}}[\tilde{\rho}_l(1-\alpha)(\tilde{Q}_l+\tilde{Q}_g+\tilde{c}_l\tilde{T}_l)+\tilde{\rho}_g\alpha(\tilde{Q}_gY+\tilde{c}_g\tilde{T}_g)]$$

$$+\frac{\partial}{\partial\tilde{x}}[\tilde{\rho}_l\tilde{u}_l(1-\alpha)(\tilde{Q}_l+\tilde{Q}_g+\tilde{c}_l\tilde{T}_l)+\tilde{\rho}_g\tilde{u}_g\alpha(\tilde{Q}_gY+\tilde{c}_g\tilde{T}_g)]$$

$$=\frac{\partial}{\partial\tilde{x}}\left[\tilde{\lambda}_l(1-\alpha)\frac{\partial\tilde{T}_l}{\partial\tilde{x}}+\tilde{\lambda}_g\alpha\frac{\partial\tilde{T}_g}{\partial\tilde{x}}+\tilde{Q}_g\tilde{\rho}_g\tilde{D}\alpha\frac{\partial Y}{\partial\tilde{x}}\right]+\alpha\frac{\partial\tilde{\rho}_g}{\partial\tilde{t}},\quad \tilde{x}>\tilde{x}_m. \tag{8}$$

In the reactionless solid/gas region, conservation of energy may thus be written in the form

$$\frac{\partial}{\partial\tilde{t}}[\tilde{\rho}_s\tilde{c}_s(1-\alpha_s)\tilde{T}_s]-\frac{\partial}{\partial\tilde{x}}\left[\tilde{\lambda}_s(1-\alpha_s)\frac{\partial\tilde{T}_s}{\partial\tilde{x}}\right]=\tilde{K}_{sg}(\tilde{T}_g-\tilde{T}_s),\quad \tilde{x}<\tilde{x}_m, \tag{9}$$

$$\frac{\partial}{\partial\tilde{t}}[\tilde{\rho}_s\tilde{c}_s(1-\alpha_s)\tilde{T}_s+\tilde{\rho}_g\tilde{c}_g\alpha_s\tilde{T}_g]+\frac{\partial}{\partial\tilde{x}}(\tilde{\rho}_g\tilde{c}_g\tilde{u}_g\alpha_s\tilde{T}_g)$$

$$=\frac{\partial}{\partial\tilde{x}}\left[\tilde{\lambda}_s(1-\alpha_s)\frac{\partial\tilde{T}_s}{\partial\tilde{x}}+\tilde{\lambda}_g\alpha_s\frac{\partial\tilde{T}_g}{\partial\tilde{x}}\right]+\alpha_s\frac{\partial\tilde{p}_g}{\partial\tilde{t}},\quad \tilde{x}<\tilde{x}_m, \tag{10}$$

where (10) describes overall energy conservation which we obtain by summing Equation (9) for the solid and the corresponding equation for the gas phase.

As described in previous work ([4], [7]), analogous equations may be written for momentum conservation (see below), but they do not need to be introduced explicitly for the present class of deflagration-type problems. As remarked above, the approximation of small Mach number implies that the gas pressure $\tilde{p}_g$, which is coupled to the other field variables through the gas-phase equation of state, is independent of the spatial coordinate. In the present work, the gas is assumed to be ideal, whence

$$\tilde{p}_g=\tilde{\rho}_g(Y/\tilde{W}_I+(1-Y)/\tilde{W}_P)\tilde{R}^\circ\tilde{T}_g, \tag{11}$$

where $\tilde{W}_I$ and $\tilde{W}_P$ are the respective molecular weights of the intermediate and product gases.

Aside from initial and boundary conditions, which will be specified shortly, one additional equation, such as an equation for either $\tilde{u}_g$ or $\tilde{u}_l$, is required to close the above system. One possibility is to invoke the simple assumption that $\tilde{u}_g=\tilde{u}_l$, but the neglect of velocity differences between the condensed and gas phases, though characteristic of early work (see [2] and [3]), cannot account for potentially significant phenomena associated with convective enthalpy transport by the gas relative to enthalpy transport in the condensed phases [16]. Moreover, such an assumption can be shown to be inconsistent with momentum conservation. Indeed, a more careful analysis of gas and condensed-phase momentum, allowing for non-equilibrium between the gas and condensed-phase pressures, was considered in [4], where it was determined that a qualitatively correct approximation in the limit of small viscous and surface-tension-gradient forces is, for $\tilde{u}_s=0$,

$$\tilde{u}_l=\frac{-\partial\tilde{x}_m}{\partial\tilde{t}}\left[\frac{\tilde{\rho}_s}{\tilde{\rho}_l}(1-s\alpha)-1\right], \tag{12}$$

where s is a velocity-perturbation parameter that reflects the (opposing) contributions of viscous and surface-tension-gradient effects. Equation (12) is the final result needed to close the system. In the limit that viscous and surface-tension-gradient effects vanish, $s\to 0$, which,

for simplicity, is the case considered here. Some effects associated with nonzero values of this parameter were studied previously in connection with the nonporous problem ([4], [6]).

The above equations now constitute a closed set for the variables $\alpha, \tilde{u}_g, \tilde{T}_l, \tilde{T}_g, \tilde{T}_s, \tilde{\rho}_g$ and $\tilde{p}_g$. The problem is thus completely determined once initial and boundary conditions (including interface relations at $\tilde{x} = \tilde{x}_m$) are specified. In the present work, we will not be concerned with the initial-value problem, but only the long-time solution corresponding to an unconfined, steadily propagating deflagration. Thus, $\partial\tilde{p}/\partial\tilde{t} = 0$ in (8) and (10), and the required boundary conditions are given by

$$\alpha = \alpha_s \quad \text{for} \quad \tilde{x} < \tilde{x}_m, \tag{13}$$

$$\tilde{u}_g \to 0, \quad Y \to 1, \quad \tilde{T}_g \to \tilde{T}_s \to \tilde{T}_u \quad \text{as} \quad \tilde{x} \to -\infty, \tag{14}$$

$$\alpha \to 1, \quad \tilde{p}_g \to \tilde{p}_g^\circ, \quad Y \to 0, \quad \tilde{T}_l \to \tilde{T}_g \to \tilde{T}_b \quad \text{as} \quad \tilde{x} \to +\infty, \tag{15}$$

where the burned temperature $\tilde{T}_b$ is to be determined, and, since $\tilde{p}_g$ is a constant for the unconfined deflagration considered here, the boundary condition on pressure implies that $\tilde{p}_g = \tilde{p}_g^\circ$ everywhere. Finally, if $\pm$ superscripts denote quantities evaluated at $\tilde{x} = \tilde{x}_m^\pm$, the continuity and jump conditions across the melting surface are

$$\tilde{\rho}_g^- = \tilde{\rho}_g^+, \qquad Y^- = Y^+, \tag{16}$$

$$\tilde{T}_g^- = \tilde{T}_g^+, \quad \tilde{T}_s^- = \tilde{T}_l^+ \equiv \tilde{T}_m, \tag{17}$$

conservation of condensed- and gas-phase mass fluxes,

$$(1-\alpha_s)\tilde{\rho}_s\left(-\frac{\mathrm{d}\tilde{x}_m}{\mathrm{d}\tilde{t}}\right) = (1-\alpha^+)\tilde{\rho}_l\left(\tilde{u}_l^+ - \frac{\mathrm{d}\tilde{x}_m}{\mathrm{d}t}\right), \tag{18}$$

$$\alpha_s\left(\tilde{u}_g^- - \frac{\mathrm{d}\tilde{x}_m}{\mathrm{d}\tilde{t}}\right) = \alpha^+\left(\tilde{u}_g^+ - \frac{\mathrm{d}\tilde{x}_m}{\mathrm{d}\tilde{t}}\right), \tag{19}$$

$$\alpha^+\tilde{D}\left.\frac{\partial Y}{\partial\tilde{x}}\right|_{\tilde{x}=\tilde{x}_m^+} - \alpha_s\tilde{D}\left.\frac{\partial Y}{\partial\tilde{x}}\right|_{\tilde{x}=\tilde{x}_m^-} = 0, \tag{20}$$

and conservation of condensed- and gas-phase enthalpy fluxes,

$$\begin{aligned}(1-\alpha^+)\tilde{\lambda}_l\left.\frac{\partial\tilde{T}_l}{\partial\tilde{x}}\right|_{\tilde{x}=\tilde{x}_m^+} - (1-\alpha_s)\tilde{\lambda}_s\left.\frac{\partial\tilde{T}_s}{\partial\tilde{x}}\right|_{\tilde{x}=\tilde{x}_m^-} &= \tilde{\rho}_s\tilde{\gamma}_s(1-\alpha_s)\frac{\mathrm{d}\tilde{x}_m}{\mathrm{d}\tilde{t}} \\ &+ \left[\tilde{\rho}_l\tilde{c}_l(1-\alpha^+)\left(\tilde{u}_l^+ - \frac{\mathrm{d}\tilde{x}_m}{\mathrm{d}\tilde{t}}\right) - \tilde{\rho}_s\tilde{c}_s(1-\alpha_s)\left(-\frac{\mathrm{d}\tilde{x}_m}{\mathrm{d}\tilde{t}}\right)\right]\tilde{T}_m,\end{aligned} \tag{21}$$

$$\alpha^+\tilde{\lambda}_g\left.\frac{\partial\tilde{T}_g}{\partial\tilde{x}}\right|_{\tilde{x}=\tilde{x}_m^+} - \alpha_s\tilde{\lambda}_g\left.\frac{\partial\tilde{T}_g}{\partial\tilde{x}}\right|_{\tilde{x}=\tilde{x}_m^-} = 0, \tag{22}$$

where $\tilde{\gamma}_s$ is the heat of melting of the solid at temperature $\tilde{T} = 0$ ($\tilde{\gamma}_s$ being negative when melting is endothermic). From Equations (12), (18) and (19) we obtain the relations

$$\alpha^+\tilde{u}_g^+ - \alpha_s\tilde{u}_g^- = -\frac{\mathrm{d}\tilde{x}_m}{\mathrm{d}\tilde{t}}(\alpha_s - \alpha^+), \quad \alpha_s - \alpha^+ = s\alpha^+(1-\alpha^+). \tag{23–24}$$

Consequently, in the limit $s = 0$ considered here, (23)–(24) reduce to the statement that $\alpha = \alpha_s$ and $\tilde{u}_g$ are continuous across $\tilde{x} = \tilde{x}_m$. Hence, from (20) and (22), $\partial Y/\partial\tilde{x}$ and $\partial\tilde{T}_g/\partial\tilde{x}$ are continuous there as well, and (21) reduces to

$$\tilde{\lambda}_l \left.\frac{\partial\tilde{T}_l}{\partial\tilde{x}}\right|_{\tilde{x}=\tilde{x}_m^+} - \tilde{\lambda}_s \left.\frac{\partial\tilde{T}_s}{\partial\tilde{x}}\right|_{\tilde{x}=\tilde{x}_m^-} = \tilde{\rho}_s \frac{\mathrm{d}\tilde{x}_m}{\mathrm{d}\tilde{t}}[\tilde{\gamma}_s + (\tilde{c}_s - \tilde{c}_l)\tilde{T}_m], \quad s = 0. \tag{25}$$

3. Dimensionless formulation of the steady-state problem

In the present work, we will confine our attention to the case of a steadily propagating deflagration that propagates with the (unknown) speed $\tilde{U} = -\mathrm{d}\tilde{x}_m/\mathrm{d}\tilde{t}$, which is a convenient characteristic velocity for the problem. Assuming constant values for heat capacities and thermal conductivities, we then introduce the nondimensional variables

$$x = \frac{\tilde{\rho}_s\tilde{c}_s\tilde{U}}{\tilde{\lambda}_s}\tilde{x}, \quad t = \frac{\tilde{\rho}_s\tilde{c}_s\tilde{U}^2}{\tilde{\lambda}_s}\tilde{t}, \quad T_{s,l,g} = \frac{\tilde{T}_{s,l,g}}{\tilde{T}_u}, \quad u_{l,g} = \frac{\tilde{u}_{l,g}}{\tilde{U}}, \quad \rho_g = \frac{\tilde{\rho}_g}{\tilde{\rho}_g^u}, \tag{26}$$

where, from the equation of state (11) evaluated at $x = -\infty$ according to (14), the upstream reference gas density $\tilde{\rho}_g^u$ is defined as $\tilde{\rho}_g^u = \tilde{p}_g^\circ\tilde{W}_I/\tilde{R}^\circ\tilde{T}_u$. In addition, the nondimensional parameters

$$r = \frac{\tilde{\rho}_l}{\tilde{\rho}_s}, \quad \hat{r} = \frac{\tilde{\rho}_g^u}{\tilde{\rho}_s}, \quad l = \frac{\tilde{\lambda}_l}{\tilde{\lambda}_s}, \quad \hat{l} = \frac{\tilde{\lambda}_g}{\tilde{\lambda}_s}, \quad b = \frac{\tilde{c}_l}{\tilde{c}_s}, \quad \hat{b} = \frac{\tilde{c}_g}{\tilde{c}_s}, \quad \gamma_s = \frac{\tilde{\gamma}_s}{\tilde{c}_s\tilde{T}_u}, \quad w = \frac{\tilde{W}_I}{\tilde{W}_P},$$

$$Le = \frac{\tilde{\lambda}_g}{\tilde{\rho}_g\tilde{D}\tilde{c}_g}, \quad Q_l = \frac{\tilde{Q}_l}{\tilde{c}_s\tilde{T}_u}, \quad Q_g = \frac{\tilde{Q}_g}{\tilde{c}_s\tilde{T}_u}, \quad N_l = \frac{\tilde{E}_l}{\tilde{R}^\circ\tilde{T}_b}, \quad N_g = \frac{\tilde{E}_g}{\tilde{R}^\circ\tilde{T}_b}, \tag{27}$$

$$K_{sg} = \frac{\tilde{\lambda}_s\tilde{K}_{sg}}{\tilde{\rho}_s^2\tilde{c}_s^2\tilde{U}^2}, \quad K_{lg} = \frac{\tilde{\lambda}_s\tilde{K}_{lg}}{rb\tilde{\rho}_s^2\tilde{c}_s^2\tilde{U}^2}, \quad \Lambda_l = \frac{\tilde{\lambda}_s\tilde{A}_l}{\tilde{\rho}_s\tilde{c}_s\tilde{U}^2}e^{-N_l}, \quad \Lambda_g = \frac{\tilde{\lambda}_s\tilde{A}_g(\tilde{\rho}_g^u)^n}{\tilde{\rho}_s^2\tilde{c}_s\tilde{U}^2}e^{-N_g},$$

are defined, where n is the reaction order of the gas-phase reaction and *Le* is the Lewis number associated with the gas phase. Having assumed a constant value for $\tilde{\lambda}_g$, we also assume that $\tilde{\rho}_g\tilde{D}$ is constant, which implies a constant Lewis number. Finally, we remark that either Λ_l or Λ_g may be regarded as an appropriate burning-rate eigenvalue, since the determination of either provides an expression for the propagation speed $\tilde{U}$. Indeed, since $\Lambda_g/\Lambda_l = \hat{r}(\tilde{A}_g/\tilde{A}_s)(\tilde{\rho}_g^u)^{n-1}e^{N_l-N_g}$, we shall, for definiteness, regard Λ_l as the burning-rate eigenvalue.

To analyze the case of a steadily propagating deflagration, it is convenient to transform to the moving coordinate $\xi = x + t$ whose origin is defined to be x_m. Introducing the above nondimensionalizations and coordinate transformation into the problem formulated in the previous section, we obtain, after setting time derivatives to zero, the steady eigenvalue problem

$$\frac{\mathrm{d}}{\mathrm{d}\xi}[\rho_g(u_g + 1)] = 0, \quad \xi < 0, \tag{28}$$

$$\frac{\mathrm{d}}{\mathrm{d}\xi}[\hat{r}\rho_g Y(u_g+1)] = \frac{\hat{l}}{\hat{b}} Le^{-1} \frac{\mathrm{d}^2 Y}{\mathrm{d}\xi^2}, \quad \xi < 0, \tag{29}$$

$$\frac{\mathrm{d}}{\mathrm{d}\xi}[r(1-\alpha)(u_l+1) + \hat{r}\alpha\rho_g(u_g+1)] = 0, \quad \xi > 0, \tag{30}$$

$$\frac{\mathrm{d}}{\mathrm{d}\xi}[\hat{r}\alpha\rho_g Y(u_g+1) + r(1-\alpha)(u_l+1)]$$

$$= \frac{\hat{l}}{\hat{b}} Le^{-1} \frac{\mathrm{d}}{\mathrm{d}\xi}\left(\alpha \frac{dY}{d\xi}\right) - \Lambda_g(\alpha\rho_g Y)^n \exp[N_g(1-T_b/T_g)], \quad \xi > 0, \tag{31}$$

$$\frac{\mathrm{d}}{\mathrm{d}\xi}[(1-\alpha)(u_l+1)] = -\Lambda_l(1-\alpha)\exp[N_l(1-T_b/T_l)], \quad \xi > 0, \tag{32}$$

$$(1-\alpha_s)\left(\frac{\mathrm{d}T_s}{\mathrm{d}\xi} - \frac{\mathrm{d}^2 T_s}{\mathrm{d}\xi^2}\right) = K_{sg}(T_g - T_s), \quad \xi < 0, \tag{33}$$

$$(1-\alpha_s)\frac{\mathrm{d}T_s}{\mathrm{d}\xi} + \hat{r}\hat{b}\alpha_s \frac{\mathrm{d}}{\mathrm{d}\xi}[\rho_g(u_g+1)T_g] = \frac{\mathrm{d}}{\mathrm{d}\xi}\left[(1-\alpha_s)\frac{\mathrm{d}T_s}{\mathrm{d}\xi} + \hat{l}\alpha_s \frac{\mathrm{d}T_g}{\mathrm{d}\xi}\right], \quad \xi < 0, \tag{34}$$

$$\frac{\mathrm{d}}{\mathrm{d}\xi}[(1-\alpha)(u_l+1)(Q_l + bT_l)] = \frac{l}{r}\frac{\mathrm{d}}{\mathrm{d}\xi}\left[(1-\alpha)\frac{\mathrm{d}T_l}{\mathrm{d}\xi}\right] + bK_{lg}(T_g - T_l), \quad \xi > 0, \tag{35}$$

$$\frac{\mathrm{d}}{\mathrm{d}\xi}[r(1-\alpha)(u_l+1)(Q_l + Q_g + bT_l) + \hat{r}\alpha\rho_g(u_g+1)(Q_g Y + \hat{b}T_g)]$$

$$= \frac{\mathrm{d}}{\mathrm{d}\xi}\left[l(1-\alpha)\frac{\mathrm{d}T_l}{\mathrm{d}\xi} + \hat{l}\alpha\frac{\mathrm{d}T_g}{\mathrm{d}\xi} + Q_g\frac{\hat{l}}{\hat{b}}Le^{-1}\alpha\frac{\mathrm{d}Y}{\mathrm{d}\xi}\right], \quad \xi > 0, \tag{36}$$

$$\rho_g T_g[Y + w(1-Y)] = 1, \quad u_l = (1-r)/r, \tag{37–38}$$

subject to the boundary conditions

$$\alpha = \alpha_s \quad \text{for } \xi \le 0, \tag{39}$$

$$u_g \to 0, \quad Y \to 1, \quad T_g \to T_s \to 1 \quad \text{as } \xi \to -\infty, \tag{40}$$

$$\alpha \to 1, \quad Y \to 0, \quad T_l \to T_g \to T_b \quad \text{as } \xi \to +\infty, \tag{41}$$

and the melting-surface ($\xi = 0$) conditions

$$T_s^- = T_l^+ = T_m, \quad T_g\Big|_{\xi=0^-}^{\xi=0^+} = u_g\Big|_{\xi=0^-}^{\xi=0^+} = Y\Big|_{\xi=0^-}^{\xi=0^+} = \frac{\mathrm{d}Y}{\mathrm{d}\xi}\Big|_{\xi=0^-}^{\xi=0^+} = \frac{\mathrm{d}T_g}{\mathrm{d}\xi}\Big|_{\xi=0^-}^{\xi=0^+} = 0, \tag{42}$$

$$l\frac{\mathrm{d}T_l}{\mathrm{d}\xi}\Big|_{\xi=0^+} - \frac{\mathrm{d}T_s}{\mathrm{d}\xi}\Big|_{\xi=0^-} = -\gamma_s + (b-1)T_m. \tag{43}$$

We remark that in writing Equations (38)–(43), we have for simplicity, set the velocity-perturbation parameter s introduced in Equation (12) to zero, implying continuity of α and u_g at $\xi = 0$ as indicated above. Thus, the final model for steady, planar deflagration that has been derived is given by (28)–(43), with the final burned temperature T_b and the flame-speed eigenvalue (either Λ_l or Λ_g) to be determined. The latter then determines the burning rate, and is the main result to be determined from the analysis that follows. We note that this model, since it allows for temperature differences between phases at a given spatial location, is sometimes referred to as a two-temperature model. An important special case, to which the present work will ultimately be restricted, is that in which the rate of interphase heat transfer, as reflected in the values of the parameters K_{sg} and K_{lg}, is large. This restriction then leads to a somewhat simpler single-temperature model as a formal first approximation to the problem defined by (28)–(43), while still allowing for the essential two-phase-flow effects associated with velocity differences between phases.

4. Determination of T_b

The solution in the region $\xi < 0$, where chemical activity has been assumed to be absent, as well as expressions for T_b and $u_{g,\infty} \equiv u_g|_{\xi=\infty}$, are obtained from the general two-temperature model as follows. From (28) and (40), we have

$$\rho_g(u_g + 1) = 1, \quad \xi < 0, \tag{44}$$

while an integration of (29) gives, upon use of (44), the integral

$$Y - 1 = \frac{\hat{l}}{\hat{r}\hat{b}}\, Le^{-1}\frac{\mathrm{d}Y}{\mathrm{d}\xi}, \quad \xi < 0. \tag{45}$$

Similarly, integration of (30) implies

$$(1 - \alpha) + \hat{r}\alpha\rho_g(u_g + 1) = \hat{r}\rho_g^b(u_{g,\infty} + 1), \quad \xi > 0, \tag{46}$$

where $\rho_g^b = (wT_b)^{-1}$ is the burned gas density. Thus, evaluating (46) at $\xi = 0$, using (44) and the fact that all variables are continuous there, we obtain an expression for the burned-gas velocity $u_{g,\infty}$ as follows

$$u_{g,\infty} = \frac{1 + \alpha_s(\hat{r} - 1)}{\hat{r}\rho_g^b} - 1, \tag{47}$$

or, in terms of T_b,

$$u_{g,\infty} = \frac{1 + \alpha_s(\hat{r} - 1)}{\hat{r}} wT_b - 1. \tag{48}$$

Turning attention to the overall energy equations (34) and (36), we may readily perform a single integration on each using the preceding results to obtain

$$(1 - \alpha_s)(T_s - 1) + \hat{r}\hat{b}\alpha_s(T_g - 1) = (1 - \alpha_s)\frac{\mathrm{d}T_s}{\mathrm{d}\xi} + \hat{l}\alpha_s\frac{\mathrm{d}T_g}{\mathrm{d}\xi}, \quad \xi < 0, \tag{49}$$

and

$$(1-\alpha)(Q_l+Q_g+bT_l)+[\alpha+\alpha_s(\hat{r}-1)](Q_gY+\hat{b}T_g)$$
$$=l(1-\alpha)\frac{\mathrm{d}T_l}{\mathrm{d}\xi}+\hat{l}\alpha\frac{\mathrm{d}T_g}{\mathrm{d}\xi}+Q_g\frac{\hat{l}}{\hat{b}}Le^{-1}\alpha\frac{\mathrm{d}Y}{\mathrm{d}\xi}+\hat{b}[1+\alpha_s(\hat{r}-1)]T_b,\quad \xi>0. \tag{50}$$

Thus, subtracting (49) evaluated at $\xi=0^-$ from (50) evaluated at $\xi=0^+$ and using the melting-surface conditions (42) and (43), we derive for T_b the expression

$$T_b=\frac{(1-\alpha_s)(Q_l+Q_g+1+\gamma_s)+\hat{r}\alpha_s(Q_g+\hat{b})}{\hat{b}[1+\alpha_s(\hat{r}-1)]}. \tag{51}$$

We note that this result has been derived from the more general two-temperature model (28)–(43) and is independent of the particular form of the equation of state for the gas. In the limit $Q_g\to 0$, Equation (51) collapses to the result obtained for the corresponding single-step model analyzed in [7].

The formulas for T_b and $u_{g,\infty}$ given above exhibit certain features worth noting. In particular, there are significant variations of the final burned temperature and gas velocity with pressure, since these quantities depend on the gas-to-solid density ratio $\hat{r}$, which in turn is proportional to $\tilde{p}_g^\circ$ according to $\hat{r}\equiv\tilde{\rho}_g^u/\tilde{\rho}_s=\tilde{W}_I\tilde{p}_g^\circ/\tilde{\rho}_s\tilde{R}^\circ\tilde{T}_u=\tilde{p}_g^\circ/\tilde{\rho}_s\tilde{c}_g(1-\gamma^{-1})\tilde{T}_u$, where γ is the ratio of specific heats for the gas. As discussed previously in connection with the single-step model ([7]), this important effect arises from the thermal expansion of the gas and the two-phase nature of the flow in the solid/gas and liquid/gas regions, where significant gas-phase convective transport of enthalpy relative to the condensed phase occurs. In the limit $\tilde{p}_g^\circ\to 0$ (*i.e.* $\hat{r}\to 0$), we see that $u_{g,\infty}\to\infty$ and $T_b\to T_b^0\equiv\hat{b}^{-1}(Q_l+Q_g+1+\gamma_s)$. Since there is effectively no gas-phase enthalpy content in this limit, T_b^0 is also the value of T_b in the limit of zero porosity ($\alpha_s\to 0$). For nonzero values of both pressure and porosity, some of the heat released by combustion must be used to help raise the temperature of the gas-phase intermediates within the porous solid from unity to T_b. Consequently, both T_b and the final gas velocity $u_{g,\infty}$ are typically decreasing functions of the nondimensional gas-phase density $\hat{r}$, which increases with pressure according to the above relation. For example, when $\hat{r}$ is relatively small, we have

$$\frac{T_b}{T_b^0}=1-\frac{\hat{r}\alpha_s}{1-\alpha_s}\left(1-\frac{Q_g+\hat{b}}{Q_l+Q_g+1+\gamma_s}\right)+O\left(\frac{\hat{r}\alpha_s}{1-\alpha_s}\right)^2, \tag{51$'$}$$

where, under typical practical circumstances, the ratio $(Q_g+\hat{b})/(Q_l+Q_g+1+\gamma_s)$ is less than unity (*e.g.*, when $\hat{b}\leqslant 1$ and $Q_l>|\gamma_s|$). An additional effect that is revealed by the two-step reaction mechanism is that T_b does not depend just on the total heat release $Q_l+Q_g\equiv Q$ associated with the complete conversion of the energetic solid to final gas products, but also on the heat release Q_g specifically associated with the gas-phase reaction. This, too, is a two-phase-flow effect that arises from the fact that the reactive intermediate gas-pase species occupy the voids in the porous solid, and the heat released by these pre-existing intermediates affects the final burned temperature. In particular, for a given total heat release Q, the burned temperature increases as the fractional heat release associated with the gas-phase reaction

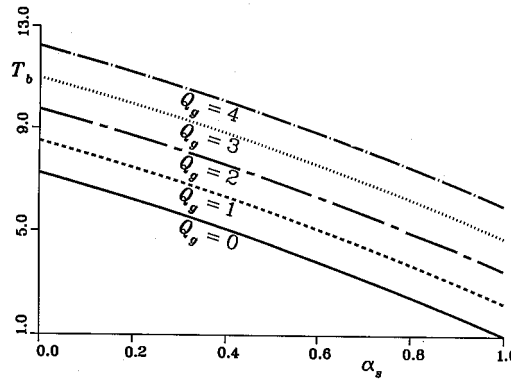

Figure 2. Final burned temperature T_b as a function of the solid porosity α_s, for several values of the gas-phase heat release Q_g (remaining parameter values are the same as those used in Figure 1).

increases. Plots of T_b as a function of α_s for several different values of Q_g are shown in Figure 2.

5. The single-temperature limit and the outer solution

As indicated at the end of section 3, an important and realistic limiting case, which results in further simplification, is to consider the formal limit of infinitely fast interphase heat transfer (*i.e.* $K_{sg}, K_{lg} \to \infty$), where such a limit corresponds to the typical case in which a representative element of the medium (such as a gas bubble) is small. In that limit, Equations (33) and (35) imply that $T_s = T_g \equiv T$ in the region $\xi < 0$, and $T_l = T_g \equiv T$ in the region $\xi > 0$. The model then reduces to a single-temperature model, which is analyzed in the next two sections. However, as discussed in Section 2, the corresponding assumption of a single-velocity model is inconsistent with momentum conservation, and thus a primary feature of even the single-temperature limit is the allowance for velocity differences between coexisting phases. The case of large, but finite, values of the interphase heat-transfer coefficients, which permit separate temperatures for each phase in the reaction zone (the region where two-temperature effects first appear), was considered in [4] and [7] in connection with the single-step model for the nonporous ($\alpha_s = 0$) and porous ($\alpha_s > 0$) cases, respectively.

In the limit that K_{sg} and K_{lg} are both infinite, the model (28)–(43) reduces to a subproblem written in terms of the single temperature variable T that denotes the common temperature of all phases at a given spatial location. In particular, we obtain in this limit the reduced set of equations given by the continuity equations (28)–(32) [with T_l and T_g each replaced by T in the reaction-rate terms, and, in (30) and (32), $u_l + 1 = r^{-1}$ according to (38)], the overall energy equations (34) and (36), which, using (38), become

$$\frac{\mathrm{d}}{\mathrm{d}\xi}\{[1 - \alpha_a + \hat{r}\hat{b}\alpha_s\rho_g(u_g + 1)]T\} = \frac{\mathrm{d}}{\mathrm{d}\xi}\left[(1 - \alpha_s + \hat{l}\alpha_s)\frac{\mathrm{d}T}{\mathrm{d}\xi}\right], \quad \xi < 0, \tag{34$'$}$$

$$\begin{aligned}&\frac{\mathrm{d}}{\mathrm{d}\xi}[(1-\alpha)(Q_l + Q_g + bT) + \hat{r}\alpha\rho_g(u_g+1)(Q_gY + \hat{b}T)] \\ &\quad = \frac{\mathrm{d}}{\mathrm{d}\xi}\left\{[l(1-\alpha) + \hat{l}\alpha]\frac{\mathrm{d}T}{\mathrm{d}\xi}\right\} + Q_g\frac{\hat{l}}{\hat{b}}Le^{-1}\frac{\mathrm{d}^2Y}{\mathrm{d}\xi^2}, \quad \xi > 0,\end{aligned} \tag{36$'$}$$

and the equation of state (37) for $\rho_g(T, Y)$. These are subject to the boundary conditions (39)–(41), in which the boundary conditions on the temperature reduce to $T \to T_b$ and $T \to 1$ at $\xi = \pm\infty$, respectively, continuity of u_g, Y, $\mathrm{d}Y/\mathrm{d}\xi$ and $T = T_m$ at $\xi = 0$, and the overall jump condition

$$[l(1-\alpha_s)+\hat{l}\alpha_s]\frac{\mathrm{d}T}{\mathrm{d}\xi}\bigg|_{\xi=0^+} - (1-\alpha_s+\hat{l}\alpha_s)\frac{\mathrm{d}T}{\mathrm{d}\xi}\bigg|_{\xi=0^-} = (1-\alpha_s)[-\gamma_s+(b-1)T_m]. \qquad (43')$$

We remark that we obtain (43′), which represents overall enthalpy-flux conservation across $\xi = 0$, by multiplying (43) by $(1 - \alpha_s)$ and adding the result to the last of (42) multiplied by $\hat{l}_s$. Finally, Equations (49) and (50) become

$$(1 - \alpha_s + \hat{r}\hat{b}\alpha_s)(T - 1) = (1 - \alpha_s + \hat{l}\alpha_s)\frac{\mathrm{d}T}{\mathrm{d}\xi}, \quad \xi < 0, \qquad (52)$$

and

$$[b(1-\alpha) + \hat{b}(\alpha - \alpha_s + \alpha_s\hat{r})]T + (\alpha - \alpha_s + \alpha_s\hat{r})Q_gY = [l(1-\alpha) + \hat{l}\alpha]\frac{\mathrm{d}T}{\mathrm{d}\xi}$$

$$+Q_g\frac{\hat{l}}{\hat{b}}Le^{-1}\alpha\frac{\mathrm{d}Y}{\mathrm{d}\xi} - (1-\alpha)(Q_l + Q_g) + \hat{b}(1 - \alpha_s + \alpha_s\hat{r})T_b, \quad \xi > 0, \qquad (53)$$

which now take the place of (34′) and (36′). We may integrate (52) using the fact that $T = T_m$ at $\xi = 0$ to give an explicit expression for T in the region $\xi \leqslant 0$, but further analytical development leading to the determination of the burning rate eigenvalue requires an analysis of the reactive liquid/gas region $\xi > 0$. Equations (31), (32) and (53) constitute three equations for Y, T and α in this region, with u_g then determined from (46) along with the equation of state (37), and the eigenvalue Λ_l determined by the boundary conditions. In order to handle the Arrhenius nonlinearities in (31) and (32), we exploit the largeness of the nondimensional activation energies N_g and N_l, and consider the formal asymptotic limit $N_g, N_l \gg 1$ such that

$$\frac{N_g}{N_l} = \nu, \quad \beta \equiv (1 - T_b^{-1})N_l \gg 1, \qquad (54)$$

where ν is an O(1) parameter and the Zel'dovich number β is the large activation-energy parameter that naturally emerges in the analysis that follows. For simplicity, we shall eventually assume $\nu \approx 1$, in which case (54) implies that we are considering the regime in which the two large activation energies differ by an approximately O(1) amount. The relation (54), along with a corresponding order relation for the ratio Λ_g/Λ_l to be introduced shortly, helps to insure that both the condensed and gas-phase reactions are active in a single thin reaction zone. Departures from (54) allow for separated reaction zones (see [17]), but in the present work we shall focus on the merged case just described (see [12], [13], [14], [15]).

In the limit $\beta \to \infty$, the Arrhenius terms are exponentially small unless T is within $\mathrm{O}(1/\beta)$ of T_b. Consequently, all chemical activity is concentrated in a very thin reaction zone whose thickness is $\mathrm{O}(1/\beta)$. On the scale of the (outer) coordinate ξ, this thin region is a sheet whose location is denoted by $\xi_r = x_r - x_m$, where $x_r > x_m$. Hence, the semi-infinite liquid/gas region is comprised of a preheat zone $0 < \xi < \xi_r$) where chemical activity is exponentially

small, the thin reaction zone where the two chemical reactions are active and go to completion, and a burned region $\xi > \xi_r$. Denoting the outer solutions on either side of the reaction zone by a zero superscript, we conclude from (32) that

$$\alpha^0 = \begin{cases} \alpha_s, & \xi < \xi_r, \\ 1, & \xi > \xi_r, \end{cases} \tag{55}$$

and from (37), (44), (46) and (47),

$$u_g + 1 = \frac{\alpha - \alpha_s + \hat{r}\alpha_s}{\hat{r}\alpha}[Y + w(1-Y)]T \tag{56}$$

for all ξ. We observe that there is a jump in α^0, and hence also in u_g^0, across the reaction zone. Similarly, in obtaining the complete outer solution for Y and T, we must connect the solutions on either side of the reaction zone by deriving appropriate jump conditions across $\xi = \xi_r$. This will ultimately entail the introduction of a stretched coordinate (see below) appropriate for analyzing the inner structure within the reaction zone, whereupon an asymptotic matching of the inner and outer solutions will yield not only the aforementioned jump conditions, but also the burning-rate eigenvalue as well. In connection with this procedure, it is convenient, and physically appealing, to attempt a representation of the reaction-rate terms in (31) and (32) as delta-function distributions with respect to the outer spatial variable ξ ([12, 13]). As a result, using the results (55) and (56), we may write the governing system of equations for the outer solution variables Y^0 and T^0 as

$$\hat{r}(Y^0 - 1) = \frac{\hat{l}}{\hat{b}}\,Le^{-1}\frac{\mathrm{d}Y^0}{\mathrm{d}\xi}, \quad \xi < 0, \tag{57}$$

$$\frac{\mathrm{d}}{\mathrm{d}\xi}[(\alpha^0 - \alpha_s + \hat{r}\alpha_s)Y^0 - \alpha^0] = \frac{\hat{l}}{\hat{b}}\,Le^{-1}\frac{\mathrm{d}}{\mathrm{d}\xi}\left(\alpha^0\frac{dY^0}{d\xi}\right) - P_g\delta(\xi - \xi_r - H),\ \xi > 0, \tag{58}$$

$$\frac{1}{r}\frac{\mathrm{d}\alpha^0}{\mathrm{d}\xi} = P_l\delta(\xi - \xi_r), \quad \xi > 0, \tag{59}$$

$$(1 - \alpha_s + \hat{r}\hat{b}\alpha_s)(T^0 - 1) = (1 - \alpha_s + \hat{l}\alpha_s)\frac{\mathrm{d}T^0}{\mathrm{d}\xi}, \quad \xi < 0, \tag{60}$$

and

$$[b(1-\alpha^0) + \hat{b}(\alpha^0 - \alpha_s + \alpha_s\hat{r})]T^0 + (\alpha^0 - \alpha_s + \alpha_s\hat{r})Q_gY^0 = [l(1-\alpha^0) + \hat{l}\alpha^0]\frac{\mathrm{d}T^0}{\mathrm{d}\xi}$$

$$+Q_g\frac{\hat{l}}{\hat{b}}\,Le^{-1}\alpha^0\frac{\mathrm{d}Y^0}{\mathrm{d}\xi} - (1-\alpha^0)(Q_l + Q_g) + \hat{b}(1 - \alpha_s + \alpha_s\hat{r})T_b, \quad \xi > 0, \tag{61}$$

where P_l and P_g are the source strengths of the reaction-rate distributions placed at $\xi = \xi_r$ and $\xi = \xi_r + H$, respectively. These quantities, along with the separation distance H, are to be determined, where the ability to do so validates the delta-function representation of the reaction rates, at least to the order of analysis considered here. We note that the $O(1/\beta)$ width

of the merged reaction zone implies that H is of this order (or smaller) as well, and in fact we will eventually seek H as an expansion in inverse powers of β.

The solution of Equations (57)–(61) subject to the melting conditions at $\xi = 0$ and the boundary conditions at $\xi = \pm\infty$ is straightforward. In particular, we find that P_l and P_g are given by

$$P_l(1-\alpha_s)/r, \quad P_g = 1 - \alpha_s + \hat{r}\alpha_s, \tag{62}$$

where, for example, the first of these follows from (55) and the integral of (59) from $\xi = \xi_r^-$ to $\xi = \xi_r^+$. The outer solutions Y^0 and T^0 are then determined in terms of H as

$$Y^0(\xi) = \begin{cases} 1 - \exp[-(1-\alpha_s+\hat{r}\alpha_s)\hat{b}LeH/\hat{l}]\exp[\hat{r}\hat{b}\,Le\,(\xi-\xi_r)/\hat{l}], & \xi < \xi_r, \\ 1 - \exp[(1-\alpha_s+\hat{r}\alpha_s)\hat{b}\,Le\,(\xi-\xi_r-H)/\hat{l}], & \xi_r < \xi < \xi_r + H, \\ 0, & \xi > \xi_r + H, \end{cases} \tag{63}$$

$$T^0(\xi) = \begin{cases} 1 + (T_m - 1)\exp\left[\dfrac{1-\alpha_s+\hat{r}\hat{b}\alpha_s}{1-\alpha_s+\hat{l}\alpha_s}\xi\right], & \xi < 0, \\ B + (T_m - B)\exp\left[\dfrac{b(1-\alpha_s)+\hat{r}\hat{b}\alpha_s}{l(1-\alpha_s)+\hat{l}\alpha_s}\xi\right], & 0 < \xi < \xi_r, \\ B_1 + (T_b - B_1)\exp\left[\dfrac{\hat{b}}{\hat{l}}(1-\alpha_s+\hat{r}\alpha_s)(\xi-\xi_r-H)\right], & \xi_r < \xi < \xi_r + H, \\ T_b = B_1 + Q_g/\hat{b} & \xi > \xi_r + H, \end{cases} \tag{64}$$

where

$$B \equiv \frac{(1-\alpha_s)(1+\gamma_s)+\hat{r}\hat{b}\alpha_s}{b(1-\alpha_s)+\hat{r}\hat{b}\alpha_s}, \quad B_1 \equiv \frac{(1-\alpha_s)(Q_l+1+\gamma_s)+\hat{r}\hat{b}\alpha_s}{\hat{b}(1-\alpha_s+\hat{r}\alpha_s)}. \tag{65}$$

The location ξ_r of the reaction zone, which appears as a sheet on the scale of the outer variable ξ, is thus determined by (64) from continuity of T at $\xi = H$ as

$$\xi_r = \frac{l(1-\alpha_s)+\hat{l}\alpha_s}{b(1-\alpha_s)+\hat{r}\hat{b}\alpha_s}\log\left\{\frac{B_1 - B + (T_b - B_1)\exp[-\hat{b}(1-\alpha_s+\hat{r}\alpha_s)H/\hat{l}]}{T_m - B}\right\}. \tag{66}$$

A sketch of the outer solution is exhibited in Figure 1.

We remark that since $H \lesssim O(1/\beta)$ and the interval $\xi_r < \xi < H$ thus lies within the merged reaction zone, that portion of (63) and (64) that actually represents the outer solution is the solution for $\xi < \xi_r$ and $\xi > \xi_r + H$. Consequently, Equations (63) and (64) imply an $O(H)$ jump in the outer solutions Y^0 and T^0 across the reaction zone [*i.e.* from $\xi = \xi_r^-$ to $\xi = (\xi_r + H)^+$]. We can motivate this directly by noting that for H small, an expansion of the delta-function $\delta(\xi - \xi_r - H)$ in (58) about $H = 0$ introduces the derivative of the delta-function, $\delta'(\xi - \xi_r)$ (see [13]). The latter implies a higher order singularity (discontinuities in the variables Y^0 and T^0 themselves) at $\xi = \xi_r$ than that which occurs when H is identically zero, in which case Y^0 and T^0 are continuous and only their derivatives (*e.g.* $\mathrm{d}Y^0/\mathrm{d}\xi$ and

$\mathrm{d}T^0/\mathrm{d}\xi$) are discontinuous there. The need to allow for the possibility of such higher order discontinuities across the reaction zone either directly (see [14]) or through the introduction of generalized functions as in the present work, is one distinguishing feature of asymptotic formulations of multi-step combustion waves relative to their single-step counterparts. The actual values of these discontinuities, as we determined here by the value of the separation distance H, as well as the burning-rate eigenvalue itself, are calculated by matching the above outer solution to the inner solution of the reaction-zone problem, which we now consider.

6. Reaction-zone solutions

The determination of the burning-rate eigenvalue Λ_l and the separation distance H, as well as the spatial evolution of the variables α, u_g, Y and T within the reaction zone (which are all discontinuous on the scale of the outer variable ξ), requires an inner analysis of the chemical boundary layer that lies in the vicinity of ξ_r. We thus introduce a stretched inner variable η,

$$\eta = \beta(\xi - \xi_r), \tag{67}$$

where the Zel'dovich number $\beta \gg 1$ was defined by the second of (54). For convenience, we also define a normalized temperature variable Θ as

$$\Theta = \frac{T-1}{T_b - 1}, \tag{68}$$

and seek solutions in the form of the expansions

$$\alpha \sim \alpha_0 + \beta^{-1}\alpha_1 + \beta^{-2}\alpha_2 + \cdots, \qquad u_g \sim u_0 + \beta^{-1}u_1 + \beta^{-2}u_2 + \cdots, \tag{69–70}$$

$$Y \sim \beta^{-1}y_1 + \beta^{-2}y_2 + \cdots, \qquad \Theta \sim 1 + \beta^{-1}\theta_1 + \beta^{-2}\theta_2 + \cdots, \tag{71–72}$$

$$\Lambda_l \sim \beta(\Lambda_0 + \beta^{-1}\Lambda_1 + \beta^{-2}\Lambda_2 + \cdots), \quad H \sim \beta^{-1}h_1 + \beta^{-2}h_2 + \cdots, \tag{73–74}$$

where the coefficients in the expansion of u_g are calculated in terms of the α_i, y_i and θ_i from (56), which is also valid in the reaction zone. At this point, we also order the nondimensional rate-coefficient ratio Λ_g/Λ_l as

$$\frac{\Lambda_g}{\Lambda_l} = \hat{r}(\tilde{\rho}_g^u)^{n-1}\frac{\tilde{A}_g}{\tilde{A}_l}\exp[(1-\nu)N_l] \equiv \beta^n\lambda, \tag{75}$$

where ν is the activation-energy ratio defined by the first equation of (54) and λ is an analogous $O(1)$ parameter that defines the scaled value of the rate-coefficient ratio. The scaling embodied in (75) is required, given (54), to construct an inner solution that corresponds to a merged reaction zone. As discussed below (54), different scalings are permissible, but would generally correspond to separated reaction zones for the condensed- and gas phase reactions (see [5]).

Substituting the above inner expansions in (31), (32) and (53), we find that the governing equations for the leading-order inner variables α_0, y_1 and θ_1 are given by

$$\frac{\mathrm{d}\alpha_0}{\mathrm{d}\eta} = r\Lambda_0(1-\alpha_0)e^{\theta_1}, \tag{76}$$

$$[l + (\hat{l} - l)\alpha_0]\frac{\mathrm{d}\theta_1}{\mathrm{d}\eta} + \frac{\hat{l}Q_g}{\hat{b}\,Le\,(T_b - 1)}\alpha_0\frac{\mathrm{d}y_1}{\mathrm{d}\eta} = \frac{(b - \hat{b})T_b + Q_l + Q_g}{T_b - 1}(1 - \alpha_0), \tag{77}$$

$$\frac{\hat{l}}{\hat{b}}\,Le^{-1}\frac{\mathrm{d}}{\mathrm{d}\eta}\left(\alpha_0\frac{\mathrm{d}y_1}{\mathrm{d}\eta}\right) = -\frac{\mathrm{d}\alpha_0}{\mathrm{d}\eta} + \lambda(wT_b)^{-n}\Lambda_0(\alpha_0 y_1)^n e^{\nu\theta_1}. \tag{78}$$

Solutions to these inner equations as $\eta \to \pm\infty$ must match with the outer solution (55), (63) and (64) as $\xi \uparrow \xi_r^-$ and as $\xi \downarrow (\xi_r + H)^+$, respectively. This leads to the matching conditions

$$\alpha_0 \to 1, \quad \theta_1 \to 0, \quad y_1 \to 0 \quad \text{as} \quad \eta \to +\infty, \tag{79}$$

and

$$\alpha_0 \to \alpha_s, \quad \theta_1 \sim E_1\eta + E_2 h_1, \quad y_1 \sim \frac{\hat{b}}{\hat{l}}\,Le\,[-\hat{r}\eta + (1 - \alpha_s + \hat{r}\alpha_s)h_1]\,\text{as}\,\eta - \infty, \tag{80}$$

where the coefficients E_1 and E_2 in the second equation of (80) are defined as

$$E_1 = \frac{T_b - B}{T_b - 1}\cdot\frac{b(1 - \alpha_s) + \hat{r}\hat{b}\alpha_s}{l(1 - \alpha_s) + \hat{l}\alpha_s}, \quad E_2 = -\frac{T_b - B_1}{T_b - 1}\cdot\frac{\hat{b}}{\hat{l}}(1 - \alpha_s + \hat{r}\alpha_s). \tag{81}$$

Solution of the complete inner problem given by (76)–(81) will only be possible for certain values of h_1 and Λ_0, which thus play the role of eigenvalues. The determination of Λ_0, the scaled leading-order coefficient in the expansion of the burning rate eigenvalue, is the main result to be obtained from the analysis that follows.

We simplify the problem defined by (76)–(81) somewhat by employing α_0 as the independent variable. Thus, using (76), we may write the remaining Equations (77) and (78) as

$$[l + (\hat{l} - l)\alpha_0]e^{\theta_1}\frac{\mathrm{d}\theta_1}{\mathrm{d}\alpha_0} + \frac{\hat{l}Q_g}{\hat{b}\,Le\,(T_b - 1)}\alpha_0 e^{\theta_1}\frac{\mathrm{d}y_1}{\mathrm{d}\alpha_0} = \frac{(b - \hat{b})T_b + Q_l + Q_g}{(T_b - 1)r\Lambda_0}, \tag{82}$$

$$r\Lambda_0\frac{\hat{l}}{\hat{b}}\,Le^{-1}\frac{\mathrm{d}}{\mathrm{d}\alpha_0}\left[\alpha_0(1 - \alpha_0)\,\mathrm{e}^{\theta_1}\frac{\mathrm{d}y_1}{\mathrm{d}\alpha_0}\right] = -1 + \frac{\lambda}{r}(wT_b)^{-n}\frac{(\alpha_0 y_1)^n}{1 - \alpha_0}\,\mathrm{e}^{(\nu-1)\theta_1}. \tag{83}$$

Since a closed-form solution to this system is not readily apparent, we restrict further analytical development to a perturbation analysis of (82) and (83) in the limit that Q_g is small relative to Q_l, corresponding to the assumption that most of the heat release occurs in the first stage of the two-step reaction process. We remark, however, that this implies that at least some of the initial exothermic gas-phase decomposition reactions should be bumped with the overall reaction (1a), regarding the resulting decomposition products as the gas-phase intermediates $I(g)$. Thus, we formally define the small parameter $\epsilon \equiv Q_g$, where $O(\beta^{-1}) \ll \epsilon \ll O(1)$, and seek solutions to the leading-order inner problem in the form

$$\alpha_0 \sim \alpha_0^0 + \epsilon\alpha_0^1 + \epsilon^2\alpha_0^2 + \cdots, \quad y_1 \sim y_1^0 + \epsilon y_1^1 + \epsilon^2 y_1^2 + \cdots, \tag{84–85}$$

$$\theta_1 \sim \theta_1^0 + \epsilon\theta_1^1 + \epsilon^2\theta_1^2 + \cdots, \quad \Lambda_0 \sim \Lambda_0^0 + \epsilon\Lambda_0^1 + \epsilon^2\Lambda_0^2 + \cdots, \tag{86–87}$$

$$h_1 \sim h_1^0 + \epsilon h_1^1 + \epsilon^2 h_1^2 + \cdots. \tag{88}$$

In addition, we observe from the expression for T_b in (64) that $T_b = B_1 + \epsilon/\hat{b}$.

Substituting these latest expansions in (82) and (83), we readily see that a subproblem for α_0^0 and θ_1^0 decouples from the full leading-order problem (with respect to ϵ), and that it is identical in form to that obtained for the single-step analysis corresponding to the global reaction scheme $R(c) \to P(g)$ ([7]). In particular, we obtain from (76) and (82)

$$[l + (\hat{l} - l)\alpha_0^0]\, \mathrm{e}^{\theta_1^0} \frac{\mathrm{d}\theta_1^0}{\mathrm{d}\alpha_0^0} = \frac{(b - \hat{b})B_1 + Q_l}{(B_1 - 1)r\Lambda_0^0}, \tag{89}$$

$$\frac{\mathrm{d}\alpha_0^0}{\mathrm{d}\eta} = r\Lambda_0^0(1 - \alpha_0^0)\, \mathrm{e}^{\theta_1^0}, \tag{90}$$

subject to

$$\begin{aligned} &\alpha_0^0 \to 1, \quad \theta_1^0 \to 0 \quad \text{as} \quad \eta + \infty, \\ &\alpha_0^0 \to \alpha_s, \quad \theta_1^0 \sim E_1^0 \eta \quad \text{as} \quad \eta \to -\infty, \end{aligned} \tag{91}$$

where E_1^0 is given by the first equation of (81) with T_b replaced by its leading-order approximation B_1. Equation (89) is readily integrated from $\alpha_0^0 = \alpha_s$ (at $\eta = -\infty$) to any $\alpha_0^0 \leqslant 1$ (at $\eta = +\infty$) to give

$$\mathrm{e}^{\theta_1^0(\alpha_0^0)} = \frac{(b - \hat{b})B_1}{(B_1 - 1)r\Lambda_0^0} \int_{\alpha_s}^{\alpha_0^0} \frac{\mathrm{d}\bar{\alpha}}{l + (\hat{l} - l)\bar{\alpha}}. \tag{92}$$

Evaluating (92) at $\alpha_0^0 = 1$ (at which $\theta_1^0 = 0$), we thus determine the leading-order coefficient Λ_0^0 in the expansion of the burning-rate eigenvalue as

$$\Lambda_0^0 = \begin{cases} \dfrac{(b - \hat{b})B_1 + Q_l}{(B_1 - 1)r(\hat{l} - l)} \log\left[\dfrac{\hat{l}}{l + (\hat{l} - l)\alpha_s}\right], & l \neq \hat{l}, \\ \dfrac{(b - \hat{b})B_1 + Q_l}{(B_1 - 1)rl}(1 - \alpha_s), & l = \hat{l}. \end{cases} \tag{93}$$

Substituting this result in (92) for arbitrary α_0 and performing the indicated integrarion, we thus obtain

$$\theta_1^0(\alpha_0^0) = \begin{cases} \log\left(\dfrac{\log[l + (\hat{l} - l)\alpha_0^0] - \log[l + (\hat{l} - l)\alpha_s]}{\log\hat{l} - \log[l + (\hat{l} - l)\alpha_s]}\right), & \hat{l} \neq l, \\ \log\left(\dfrac{\alpha_0^0 - \alpha_s}{1 - \alpha_s}\right), & \hat{l} = l. \end{cases} \tag{94}$$

The determination of $\alpha_0^0(\eta)$, and hence $\theta_1^0(\eta)$, then follows directly from (90). For example, when $\hat{l} = l$ (equal gas and liquid thermal conductivities), we obtain

$$\alpha_0^0(\eta) = \frac{\alpha_s + \exp\{l^{-1}[(b - \hat{b})B_1 + Q_l](1 - \alpha_s)\eta/(B_1 - 1)\}}{1 + \exp\{l^{-1}[(b - \hat{b})B_1 + Q_l](1 - \alpha_s)\eta/(B_1 - 1)\}}, \tag{95}$$

where the second of the matching conditions (91) has been used to evaluate the constant of integration.

The first approximation, Equation (93), for the burning-rate eigenvalue is independent of the effects of the second reaction (1b), which has been assumed to have a relatively small thermal effect. Consequently, the first effects of the two-step mechanism on the burning rate appear at $O(\epsilon)$, which, from (87), requires the calculation of Λ_0^1. We thus proceed by first calculating the leading-order mass fraction variable y_1^0, which is determined from the leading-order version of (83). For additional simplicity, we restrict further consideration to the parameter regime

$$\alpha_s = \alpha_s^1 \epsilon, \quad \hat{l} = l + \epsilon \hat{l}^1, \quad \nu = 1 + \epsilon \nu^1, \tag{96}$$

corresponding to $O(\epsilon)$ values of the initial porosity, $O(\epsilon)$ differences in the conductivities of the condensed and gaseous phases, and $O(\epsilon\beta)$ differences in the activation energies of the two reaction steps. In addition, we consider only the case of a first-order gas-phase reaction (*i.e.* $n = 1$), and assume that

$$\frac{\lambda}{rw\Lambda_0^0 T_b^0} \cdot \frac{\hat{b}\, Le}{rl} = 1 + \epsilon\lambda_1, \tag{97}$$

where $T_b^0 = (Q_l + 1 + \gamma_s)/\hat{b}$ is the leading-order approximation to T_b with respect to ϵ in the above parameter regime. The parameter group on the left-hand side of Equation (97) is a gas-to-liquid ratio of diffusion-weighted reaction rates, where we may interpret the latter as characteristic measures of the rate of depletion of the reacting species, taking into account both chemical reaction and, for the gas phase, species diffusion. Such quantities appear to arise naturally in the analysis of multi-step flames, and, based on the above interpretation, have been referred to as consumption rates (see [12, 13]). The fact that larger gas-phase Lewis numbers are associated with higher rates of depletion of the gaseous reactant stems from the higher concentration of this species in the reaction zone that results from smaller values of the gas-phase mass diffusivity.

In the parameter regime just outlined, the expressions (93) and (94) for θ_1^0 and Λ_0^0 simplify to

$$\theta_1^0 = \log \alpha_0^0, \quad \Lambda_0^0 = \frac{bQ_l + (b - \hat{b})(1 + \gamma_s)}{rl(Q_l + 1 + \gamma_s - \hat{b})}, \tag{98}$$

where, for $\alpha_s \sim O(\epsilon)$, Equation (95) implies

$$\alpha_0^0(\eta) = \frac{\exp(r\Lambda_0^0\eta)}{1 + \exp(r\Lambda_0^0\eta)}, \tag{99a}$$

or

$$\eta = \frac{1}{r\Lambda_0^0} \log\left(\frac{\alpha_0^0}{1 - \alpha_0^0}\right). \tag{99b}$$

Consequently, the leading-order version of Equation (78) for y_1^0 as a function of α_0^0 is given by

$$\frac{\mathrm{d}^2 y_1^0}{\mathrm{d}\alpha_0^{0^2}} + \left(\frac{2}{\alpha_0^0} - \frac{1}{1 - \alpha_0^0}\right)\frac{\mathrm{d}y_1^0}{\mathrm{d}\alpha_0^0} - \frac{y_1^0}{\alpha_0^0(1 - \alpha_0^0)^2} = -\frac{\hat{b}\; Le}{rl\Lambda_0^0} \cdot \frac{1}{(\alpha_0^0)^2(1 - \alpha_0^0)}, \tag{100}$$

subject to $y_1^0 \to 0$ as $\alpha_0^0 \to 1$ and an appropriate matching condition as $\alpha_0^0 \to 0$. The latter, however, cannot be obtained directly from (80) because that equation was derived under the assumption that $\alpha_s \neq 0$, whereas to leading order in ϵ, α_s is equal to zero. Indeed, at this order, the outer solution (63) for Y^0 has no meaning for $\xi < 0$, since there is no gaseous phase in this region at this order of approximation. To derive the appropriate matching conditions on the inner mass fraction variables y_1^0 and, for later use, y_1^1, we consider a new variable Z, defined as the mass fraction of the intermediate gas-phase species with respect to the total mass of all species, gaseous and condensed, at a given point. Thus, Z is defined in terms of the variables already introduced as

$$Z = \frac{\hat{r}\alpha\rho_g Y}{\hat{r}\alpha\rho_g + r(1-\alpha)} = \frac{\hat{r}\alpha Y}{\hat{r}\alpha + r(1-\alpha)[Y + w(1-Y)]T}, \tag{101}$$

where we have used the equation of state (37) to obtain the second equality. However, unlike Y, the variable Z is physically unambiguous in the limit that $\alpha \to 0$, where it must vanish. From (101) applied to the reaction zone, Z has the asymptotic development

$$\begin{aligned} Z &\sim \beta^{-1}\left[\frac{\hat{r}(\alpha_0^0 + \epsilon\alpha_0^1 + \cdots)(y_1^0 + \epsilon y_1^1 + \cdots)}{\hat{r}(\alpha_0^0 + \epsilon\alpha_0^1 + \cdots) + r(1 - \alpha_0^0 - \epsilon\alpha_0^1 - \cdots)w(T_b^0 + \epsilon T_b^1 + \cdots)}\right] + O(\beta^{-2}) \\ &\sim \beta^{-1}\left[\frac{\hat{r}\alpha_0^0 y_1^0}{\hat{r}\alpha_0^0 + r(1-\alpha_0^0)wT_b^0}\right] \\ &\quad + \epsilon\beta^{-1}\left\{\frac{\hat{r}(\alpha_0^0 y_1^1 + \alpha_0^1 y_1^0)}{\hat{r}\alpha_0^0 + r(1-\alpha_0^0)wT_b^0} - \frac{\hat{r}\alpha_0^0 y_1^0[(\hat{r} - rwT_b^0)\alpha_0^1 + r(1-\alpha_0^0)wT_b^1]}{[\hat{r}\alpha_0^0 + r(1-\alpha_0^0)wT_b^0]^2}\right\} + \cdots, \end{aligned} \tag{102}$$

where, from the last equation of (64) and (65) and the first equation of (96), T_b^0 and T_b^1 are defined by

$$T_b \sim T_b^0 + \epsilon T_b^1 + \cdots, \quad T_b^0 = (Q_l + 1 + \gamma_s)/\hat{b}, \quad T_b^1 = \hat{b}^{-1} - \hat{r}(T_b^0 - 1)\alpha_s^1. \tag{103}$$

On the other hand, form the outer solution (55), (63) and (64) and the fact that $\alpha_s = \epsilon\alpha_s^1$, the behavior of Z in the outer preheat region in the limit $\xi \uparrow \xi_r^-$, is, in terms of the inner variable η, given by

$$Z \sim \epsilon\beta^{-1}\frac{\hat{r}\alpha_s^1\hat{b}\,Le}{rwT_b^0 l}(-\hat{r}\eta + h_1^0). \tag{104}$$

Thus, requiring the inner expression (102) for Z to match with the outer expression (104) in the limit $\eta \to -\infty$, we equate like-order terms to arrive at the matching conditions

$$\alpha_0^0 y_1^0 \to 0 \quad \text{as} \quad \alpha_0^0 \to 0 \tag{105}$$

and

$$\alpha_0^0 y_1^1 \sim -\alpha_s^1 y_1^0 + \alpha_s^1\frac{\hat{b}\,Le}{l}\left(-\frac{\hat{r}}{r\Lambda_0^0}\log\alpha_0^0 + h_1^0\right) \quad \text{as} \quad \alpha_0^0 \to 0, \tag{106}$$

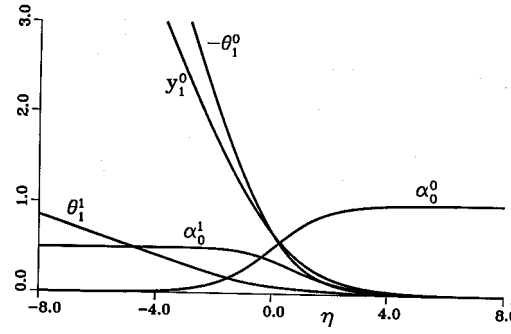

Figure 3. Inner structure of the leftward-propagating deflagration wave. Curves were drawn for the parameter regime analyzed in Section 6, based on the parameter values used in Figure 1 (the latter imply that the scaled parameters $\alpha_s^1 = \alpha_s/Q_g = 0{\cdot}5$ and $\hat{l}^1 = (\hat{l} - l)/Q_g = -0{\cdot}4$).

where we have used Equation (99b) to write these conditions in terms of α_0^0 as α_0^0 tends to zero, and have used (105) and the fact that $\alpha_0^1 \to \alpha_s^1$ in this limit to obtain the final form of (106).

Proceeding with the solution for y_1^0, we observe that homogeneous solutions of (100) are $(\alpha_0^0)^{-1}(1-\alpha_0^0)$ and $(\alpha_0^0)^{-1}(1-\alpha_0^0)^{-1}$, whence a particular solution may be constructed in a standard fashion (*e.g.*, by use of the variation of constants formula). In this way, the general soution of (100) is determined as

$$y_1^0 = c_1\frac{1-\alpha_0^0}{\alpha_0^0} + c_2\frac{1}{\alpha_0^0(1-\alpha_0^0)} - \frac{\hat{b}\,Le}{2rl\Lambda_0^0}\left[\frac{1-\alpha_0^0}{\alpha_0^0}\log\left(\frac{1-\alpha_0^0}{\alpha_0^0}\right) + \frac{\log\alpha_0^0 - \alpha_0^0}{\alpha_0^0(1-\alpha_0^0)}\right], \tag{107}$$

where c_1 and c_2 are arbitrary constants of integration. Applying the boundary condition at $\alpha_0^0 = 1$, we conclude that $c_2 = -\hat{b}\,Le/2rl\Lambda_0^0$, while requiring that the condition (105) be satisfied gives $c_1 = -c_2$. Thus, y_1^0 is given by

$$y_1^0 = -\frac{\hat{b}\,Le}{2rl\Lambda_0^0}\left[1 + \frac{1-\alpha_0^0}{\alpha_0^0}\log\left(\frac{1-\alpha_0^0}{\alpha_0^0}\right) + \frac{\log\alpha_0^0}{\alpha_0^0(1-\alpha_0^0)}\right], \tag{108}$$

which completes our analysis of the leading-order reaction-zone problem. We observe that, although $\alpha_0^0 y_1^0$ approaches zero in the limit that α_0^0 becomes small, as required by (105), the variable y_1^0 itself is unbounded in that limit, exhibiting the behavior $y_1^0 \sim -(\hat{b}\,Le/rl\Lambda_0^0)\ln\alpha_0^0$ as $\alpha_0^0 \to 0$. Profiles of the leading-order inner variables are shown in Figure 3, where the relationship (99a) for $\alpha_0^0(\eta)$ was used to exhibit these variables as functions of η.

The reaction-zone problem at the next order (with respect to ϵ) is obtained by collecting terms of order ϵ when the expansions (84)–(88), (96) and (97) are substituted in (76)–(80). This results in a problem for the inner variables α_0^1, y_1^1 and θ_1^1 introduced in Equations (84)–(86) and the coefficients Λ_0^1 and h_1^0 that appear in the corresponding expansions (87) and (88) for the eigenvalues Λ_0 and h_1. In particular, we obtain

$$\frac{\mathrm{d}\alpha_0^1}{\mathrm{d}\eta} = r[\Lambda_0^0(1-\alpha_0^0)\theta_1^1 + \Lambda_0^1(1-\alpha_0^0) - \Lambda_0^0\alpha_0^1]\,\mathrm{e}^{\theta_1^0}, \tag{109}$$

$$l\frac{\mathrm{d}\theta_1^1}{\mathrm{d}\eta} + \hat{l}^1\alpha_0^0\frac{\mathrm{d}\theta_1^0}{\mathrm{d}\eta} + \frac{l}{\hat{b}\,Le\,(T_b^0 - 1)}\alpha_0^0\frac{\mathrm{d}y_1^0}{\mathrm{d}\eta} = -C_0\alpha_0^1 + C_1(1-\alpha_0^0), \tag{110}$$

$$\frac{l}{\hat{b}}\,Le^{-1}\frac{\mathrm{d}}{\mathrm{d}\eta}\left(\alpha_0^0\frac{\mathrm{d}y_1^1}{\mathrm{d}\eta}+\alpha_0^1\frac{\mathrm{d}y_1^0}{\mathrm{d}\eta}\right)+\frac{\hat{l}^1}{\hat{b}}\,Le^{-1}\frac{\mathrm{d}}{\mathrm{d}\eta}\left(\alpha_0^0\frac{\mathrm{d}y_1^0}{\mathrm{d}\eta}\right)+\frac{\mathrm{d}\alpha_0^1}{\mathrm{d}\eta}=$$

$$\frac{r^2l\Lambda_0^0}{\hat{b}\,Le}\left[\left(\lambda_1-\frac{T_b^1}{T_b^0}\right)\Lambda_0^0+\Lambda_0^1\right]\alpha_0^0y_1^0\,\mathrm{e}^{\theta_1^0}+\frac{r^2l}{\hat{b}\,Le}(\Lambda_0^0)^2[\alpha_0^1y_1^0+\alpha_0^0y_1^1+\alpha_0^0y_1^0(\nu_1\theta_1^0+\theta_1^1)]\,\mathrm{e}^{\theta_1^0},\quad(111)$$

subject to the matching conditions

$$\alpha_0^1\to 0,\quad \theta_1^1\to 0,\quad y_1^1\to 0\quad\text{as}\quad \eta\to+\infty,\tag{112}$$

$$\alpha_0^1\to\alpha_s^1,\quad \theta_1^1\sim E_1^1\eta+E_2^1h_1^0,\quad \alpha_0^0y_1^1\sim\alpha_s^1\frac{\hat{b}\,Le}{l}[(1-\hat{r})\eta+h_1^0]\quad\text{as}\quad\eta\to-\infty,\tag{113}$$

where we have used the behavior of y_1^0 indicated below Equation (108) to simplify the matching condition (106) on $\alpha_0^0y_1^1$ as $\eta\sim(r\Lambda_0^0)^{-1}\log\alpha_0^0\to-\infty$. Here, from the last of Equations (64) and (65) and the first Equation of (96), the coefficients C_0, C_1, E_1^1 and E_2^1 are given by

$$C_0=\frac{(b-\hat{b})T_b^0+Q_l}{T_b^0-1}=rl\Lambda_0^0,\quad C_1=\frac{T_b^0-1-T_b^1(Q_l+b-\hat{b})}{(T_b^0-1)^2},\tag{114}$$

$$E_1^1=\frac{\alpha_s^1(\hat{r}\hat{b}-b)}{l}+\frac{[\alpha_s^1(T_b^0-1)+T_b^1](1+\gamma_s-b)}{l(T_b^0-1)^2},\quad E_2^1=-\frac{1}{l(T_b^0-1)},\tag{115}$$

where T_b^0 and T_b^1 were defined in (103). We observe that T_b^1, and hence C_1 and E_1^1, all depend on α_s^1, reflecting, to this order of approximation, a linearly decreasing dependence of the burned temperature on the initial porosity for small values of the latter.

It is again convenient to use a volume-fraction variable(in this case, α_0^0) as the independent variable, which transforms (109)–(111) into a somewhat simpler form. In particular, from (99), we obtain the transformation rule

$$\frac{\mathrm{d}}{\mathrm{d}\eta}=r\Lambda_0^0\alpha_0^0(1-\alpha_0^0)\frac{\mathrm{d}}{\mathrm{d}\alpha_0^0},\tag{116}$$

which, along with the expressions (98a) and (108) for θ_1^0 and y_1^0, results in the transformed system

$$\frac{\mathrm{d}\alpha_0^1}{\mathrm{d}\alpha_0^0}+\frac{\alpha_0^1}{1-\alpha_0^0}=\theta_1^1+\frac{\Lambda_0^1}{\Lambda_0^0},\tag{117}$$

$$rl\Lambda_0^0\alpha_0^0(1-\alpha_0^0)\frac{\mathrm{d}\theta_1^1}{\mathrm{d}\alpha_0^0}+C_0\alpha_0^1=C_1(1-\alpha_0^0)-r\hat{l}^1\Lambda_0^0\alpha_0^0(1-\alpha_0^0)$$
$$+\frac{1}{2(T_b^0-1)}\left[\alpha_0^0-(1-\alpha_0^0)\log(1-\alpha_0^0)+\frac{(\alpha_0^0)^2}{1-\alpha_0^0}\log\alpha_0^0\right],\tag{118}$$

$$\frac{\mathrm{d}^2 y_1^1}{\mathrm{d}\alpha_0^{0^2}} + \left(\frac{2}{\alpha_0^0} - \frac{1}{1-\alpha_0^0}\right)\frac{\mathrm{d}y_1^1}{\mathrm{d}\alpha_0^0} - \frac{y_1^1}{\alpha_0^0(1-\alpha_0^0)^2}$$

$$= \frac{\hat{b}\,Le}{2rl\Lambda_0^0}\cdot\frac{1}{(\alpha_0^0)^2(1-\alpha_0^0)}\frac{\mathrm{d}}{\mathrm{d}\alpha_0^0}\left\{\alpha_0^1\left[-1-\frac{1-\alpha_0^0}{\alpha_0^0}\log(1-\alpha_0^0)+\frac{\alpha_0^0}{1-\alpha_0^0}\log\alpha_0^0\right]\right\}$$

$$+\frac{\hat{l}^1}{l}\cdot\frac{\hat{b}\,Le}{2rl\Lambda_0^0}\cdot\frac{1}{(\alpha_0^0)^2(1-\alpha_0^0)}\left[\frac{2-\alpha_0^0}{1-\alpha_0^0}+\log(1-\alpha_0^0)+\frac{\alpha_0^0(2-\alpha_0^0)}{(1-\alpha_0^0)^2}\log\alpha_0^0\right]$$

$$-\frac{\hat{b}\,Le}{2rl\Lambda_0^0}\cdot\frac{1}{\alpha_0^0(1-\alpha_0^0)^2}\left(\lambda_1-\frac{T_b^1}{T_b^0}+\frac{\Lambda_0^1}{\Lambda_0^0}+\frac{\alpha_0^1}{\alpha_0^0}+\theta_1^1+\nu^1\log\alpha_0^0\right)$$

$$\times\left[1+\frac{1-\alpha_0^0}{\alpha_0^0}\log\left(\frac{1-\alpha_0^0}{\alpha_0^0}\right)+\frac{\log\alpha_0^0}{\alpha_0^0(1-\alpha_0^0)}\right], \tag{119}$$

subject to

$$\alpha_0^1\to 0,\quad \theta_1^1\to 0,\quad y_1^1\to 0\quad\text{as}\quad \alpha_0^0\to 1, \tag{120}$$

$$\alpha_0^1\to\alpha_s^1,\quad \theta_1^1\sim\frac{E_1^1}{r\Lambda_0^0}\log\alpha_0^0+E_2^1h_1^0,$$

$$\alpha_0^0 y_1^1\sim\alpha_s^1\frac{\hat{b}\,Le}{l}\left(\frac{l-\hat{r}}{r\Lambda_0^0}\log\alpha_0^0+h_1^0\right)\ \text{as}\quad \alpha_0^0\to 0. \tag{121}$$

Solution of the subsystem (117) and (118) for α_0^1 and θ_1^1, subject to the above matching conditions, will determine the burning rate eigenvalue Λ_0^1, while the subsequent solution of (119) for y_1^1 will, from the last matching condition in (121), determine the separation-distance coefficient h_1^0.

The solution for α_0^1 and θ_1^1 proceeds as follows. Multiplying (117) by the integrating factor $(1-\alpha_0^0)^{-1}$, we may rewrite this equation as

$$\frac{\mathrm{d}}{\mathrm{d}\alpha_0^0}\left(\frac{\alpha_0^1}{1-\alpha_0^0}\right)=\frac{1}{1-\alpha_0^0}\left(\theta_1^1+\frac{\Lambda_0^1}{\Lambda_0^0}\right), \tag{122}$$

Then, dividing (118) by $1-\alpha_0^0$ and differentiating with respect to α_0^0, we may substitute (122) in the result to obtain a single second-order equation for θ_1^1 given by

$$\frac{\mathrm{d}^2\theta_1^1}{\mathrm{d}\alpha_0^{0^2}}+\frac{1}{\alpha_0^0}\frac{\mathrm{d}\theta_1^1}{\mathrm{d}\alpha_0^0}+\frac{\theta_1^1}{\alpha_0^0(1-\alpha_0^0)}$$

$$=\frac{1}{rl\Lambda_0^0(T_b^0-1)}\left[\frac{1}{\alpha_0^0(1-\alpha_0^0)^2}+\frac{\log\alpha_0^0}{(1-\alpha_0^0)^3}\right]-\frac{\Lambda_0^1/\Lambda_0^0}{\alpha_0^0(1-\alpha_0^0)}-\frac{\hat{l}^1/l}{\alpha_0^0}, \tag{123}$$

where we have used the fact that $C_0 = rl\Lambda_0^0$. Homogeneous solutions of (123) are $1 - \alpha_0^0$ and $(1 - \alpha_0^0)\log[\alpha_0^0(1 - \alpha_0^0)^{-1}] + 1$. To obtain a particular solution, we first introduce a new variable v defined by $\theta_1^1 = (1 - \alpha_0^0)v$, where, by substituting this form of the solution in (123), we find that $\mathrm{d}v/\mathrm{d}\alpha_0^0 \equiv u$ satisfies the first-order equation

$$\frac{\mathrm{d}u}{\mathrm{d}\alpha_0^0} + \frac{1 - 3\alpha_0^0}{\alpha_0^0(1 - \alpha_0^0)}u = \frac{\mathrm{RHS}_{123}}{1 - \alpha_0^0}, \tag{124}$$

where 'RHS_{123}' denotes the inhomogeneous right-hand side of Equation (123). Multiplying Equation (124) by the integrating factor $\alpha_0^0(1 - \alpha_0^0)^2$, we may rewrite that equation as

$$\frac{\mathrm{d}}{\mathrm{d}\alpha_0^0}[\alpha_0^0(1 - \alpha_0^0)^2 u] = \alpha_0^0(1 - \alpha_0^0)(\mathrm{RHS}_{123}). \tag{125}$$

Integrating the latter, we obtain a particular integral u_p as

$$u_p = \frac{\mathrm{d}v_p}{\mathrm{d}\alpha_0^0} = \frac{1}{\alpha_0^0(1 - \alpha_0^0)^2}\left\{\frac{1}{rl\Lambda_0^0(T_b^0 - 1)}\left[\frac{\alpha_0^0}{1 - \alpha_0^0}\log\alpha_0^0 - \mathrm{Li}_2(1 - \alpha_0^0)\right]\right.$$
$$\left. - \frac{\Lambda_0^1}{\Lambda_0^0}\alpha_0^0 + \frac{\hat{l}^1}{2l}(1 - \alpha_0^0)^2\right\}, \tag{126}$$

where we have introduced the dilogarithm function $\mathrm{Li}_2(\alpha)$, which is defined for all complex α by

$$\mathrm{Li}_2(\alpha) = -\int_0^\alpha \frac{\log(1 - \bar{\alpha})}{\bar{\alpha}}\,\mathrm{d}\bar{\alpha} = \sum_{j=1}^{\infty}\frac{\alpha^j}{j^2}, \tag{127}$$

where the latter form of the representation is convergent for $|\alpha| \leqslant 1$ (see [18]). In the real domain of interest here $(0 \leqslant \alpha \leqslant 1)$, $\mathrm{Li}_2(\alpha)$ is a monotonic function that ranges from $\mathrm{Li}_2(0) = 0$ to $\mathrm{Li}_2(1) = \pi^2/6$. In what follows, it will also be convenient to introduce the trilogarithm $\mathrm{Li}_3(\alpha)$ where, generally speaking, the polylogarithms Li_n of order $n > 2$ are defined as

$$\mathrm{Li}_n(\alpha) = \int_0^\alpha \frac{\mathrm{Li}_{n-1}(\bar{\alpha})}{\bar{\alpha}}\,\mathrm{d}\bar{\alpha} = \sum_{j=1}^{\infty}\frac{\alpha^j}{j^n} \tag{128}$$

(see [18]). Thus, integrating (126), we obtain the general solution for θ_1^1 as

$$\theta_1^1 = c_1\left[1 + (1 - \alpha_0^0)\log\left(\frac{\alpha_0^0}{1 - \alpha_0^0}\right)\right] + c_2(1 - \alpha_0^0) - \frac{\Lambda_0^1}{\Lambda_0^0} + \frac{\hat{l}^1}{2l}(1 - \alpha_0^0)\log\alpha_0^0$$
$$+\frac{1}{rl\Lambda_0^0(T_b^0 - 1)}\left\{\frac{1}{2}\left[\frac{\log\alpha_0^0}{1 - \alpha_0^0} - (1 - \alpha_0^0)\log\left(\frac{\alpha_0^0}{1 - \alpha_0^0}\right) - 1\right]\right.$$
$$-\left[\frac{\pi^2}{6} + \mathrm{Li}_2(\alpha_0^0)\right](1 - \alpha_0^0)\log\alpha_0^0 + (1 - \alpha_0^0)[2\,\mathrm{Li}_3(\alpha_0^0) + \mathrm{Li}_3(1 - \alpha_0^0)]$$
$$\left. -\mathrm{Li}_2(1 - \alpha_0^0) + (1 - \alpha_0^0)\log(1 - \alpha_0^0) + \alpha_0\log\alpha_0^0\right\} \tag{129}$$

where c_1 and c_2 are constants of integration, and where we have used the identity

$$\mathrm{Li}_2(\alpha) + \mathrm{Li}_2(1-\alpha) = \frac{\pi^2}{6} - \log\alpha\log(1-\alpha) \tag{130}$$

to evaluate $\int^{\alpha_0^0} \alpha^{-1}\,\mathrm{Li}_2(1-\alpha)\,\mathrm{d}\alpha$. Applying the matching conditions (120) and (121), we thus obtain a set of relations for c_1, c_2, Λ_0^1 and h_1^0 given by

$$c_1 - \frac{\Lambda_0^1}{\Lambda_0^0} = \frac{1}{rl\Lambda_0^0(T_b^0-1)}, \qquad c_1 + \frac{\hat{l}^1}{2l} = \frac{1}{r\Lambda_0^0}\left[\frac{\pi^2}{6l(T_b^0-1)} + E_1^1\right], \tag{131–132}$$

$$c_1 + c_2 - \frac{\Lambda_0^1}{\Lambda_0^0} + \frac{h_1^0}{l(T_b^0-1)} = \frac{1}{rl\Lambda_0^0(T_b^0-1)}\left[\frac{\pi^2}{6} + \frac{1}{2} - \mathrm{Li}_3(1)\right], \tag{133}$$

where we have used the fact that $\mathrm{Li}_2(1) = \pi^2/6$ and $\mathrm{Li}_3(1) \doteq 1{\cdot}20205690$. Thus, from (131) and (132), the $O(\epsilon)$ coefficient Λ_0^1 in the expansion of the burning-rate eigenvalue is given uniquely by

$$\Lambda_0^1 = \frac{1}{rl(T_b^0-1)}\left(\frac{\pi^2}{6} - 1\right) + \frac{1}{r}E_1^1 - \frac{\hat{l}^1}{2l}\Lambda_0^0, \tag{134}$$

where E_1^1 was defined by (115), and the constants of integration c_1 and c_2 are given explicitly as

$$\begin{aligned} c_1 &= \frac{\pi^2}{6rl\Lambda_0^0(T_b^0-1)} + \frac{E_1^1}{r\Lambda_0^0} - \frac{\hat{l}^1}{2l}, \\ c_2 &= \frac{1}{rl\Lambda_0^0(T_b^0-1)}\left[\frac{\pi^2}{6} - \frac{1}{2} - \mathrm{Li}_3(1)\right] - \frac{h_1^0}{l(T_b^0-1)}, \end{aligned} \tag{135}$$

where the latter depends on h_1^0, which is still to be determined.

Having thus determined $\theta_1^1(\alpha_0^0)$ and Λ_0^1, we may readily solve (117) for α_0^1. In particular, multiplying that equation by the integrating factor $(1-\alpha_0^0)^{-1}$, we may rewrite (117) as

$$\frac{\mathrm{d}}{\mathrm{d}\alpha_0^0}\left(\frac{\alpha_0^1}{1-\alpha_0^0}\right) = \frac{1}{1-\alpha_0^0}\left(\theta_1^1 + \frac{\Lambda_0^1}{\Lambda_0^0}\right). \tag{136}$$

Substituting the previous results in the right-hand side of (136) and performing an integration, the general solution for α_0^1 is determined as

$$\begin{aligned} \alpha_0^1 \;=\; & c_3(1-\alpha_0^0) + (1-\alpha_0^0)\left[c_1\alpha_0^0\log\left(\frac{\alpha_0^0}{1-\alpha_0^0}\right) + c_2\alpha_0^0 + \frac{\hat{l}^1}{2l}(\alpha_0^0\log\alpha_0^0 - \alpha_0^0)\right] \\ & + \frac{1-\alpha_0^0}{rl\Lambda_0^0(T_b^0-1)}\left\{\left[\frac{3\alpha_0^0-2}{2(1-\alpha_0^0)} - \frac{\pi^2}{6}\right]\alpha_0^0\log\alpha_0^0 + \tfrac{1}{2}(3\alpha_0^0-1)\log(1-\alpha_0^0)\right. \\ & \left. + \mathrm{Li}_2(1-\alpha_0^0) - \alpha_0^0\log\alpha_0^0\,\mathrm{Li}_2(\alpha_0^0) + 2\alpha_0^0\,\mathrm{Li}_3(\alpha_0^0) + \alpha_0^0\,\mathrm{Li}_3(1-\alpha_0^0)\right\}, \end{aligned} \tag{137}$$

where the first term is the homogeneous solution and c_3 is the constant of integration. We observe that the matching condition (120a) as $\alpha_0^0 \to 1$ is identically satisfied by this solution, whereas the matching condition (121a) as $\alpha_0^0 \to 0$ determines c_3 as

$$c_3 = \alpha_s^1 - \frac{\pi^2}{6rl\Lambda_0^0(T_b^0 - 1)}. \tag{138}$$

Profiles of α_0^1 and θ_1^1 are exhibited in Figure 3, where the fact that, in the parameter regime considered here, $h_1^0 = 1 - \hat{r} = 0$ (see below) has been used to determine uniquely the constant of integration c_2 that appears in the expressions (129) and (137) for these variables.

Having obtained the solutions for θ_1^1 and α_0^1 as functions of α_0^0, we may now solve (119) explicitly for y_1^1 subject to the last of the matching conditions (120) and (121). Since the latter is expressed in terms of $\alpha_0^0 y_1^1$ it is convenient to introduce first the variable $z_1^1 \equiv \alpha_0^0 y_1^1$, in terms of which we may rewrite (119), using (117), as

$$\begin{aligned}
&\frac{\mathrm{d}}{\mathrm{d}\alpha_0^0}\left[\alpha_0^0(1-\alpha_0^0)\frac{\mathrm{d}z_1^1}{\mathrm{d}\alpha_0^0}\right] - \frac{\mathrm{d}}{\mathrm{d}\alpha_0^0}[(1-\alpha_0^0)z_1^1] - \frac{z_1^1}{1-\alpha_0^0} \\
&\quad = \frac{\hat{b}\,Le}{2rl\Lambda_0^0}\left\{\alpha_0^1\left[\frac{1}{\alpha_0^0} + \frac{1}{1-\alpha_0^0} + \frac{\log(1-\alpha_0^0)}{(\alpha_0^0)^2} - \frac{\log\alpha_0^0}{(1-\alpha_0^0)^2}\right]\right. \\
&\qquad - \left(\theta_1^1 + \frac{\Lambda_0^1}{\Lambda_0^0}\right)\left[\frac{1}{1-\alpha_0^0} + \frac{\log(1-\alpha_0^0)}{\alpha_0^0} + \frac{\alpha_0^0\log\alpha_0^0}{(1-\alpha_0^0)^2}\right] + 2\frac{\hat{l}^1}{l} \\
&\qquad - \left(\lambda_1 - \frac{T_b^1}{T_b^0} - \frac{\hat{l}^1}{l} + \nu^1\log\alpha_0^0\right) \\
&\qquad \left.\times\left[\frac{\alpha_0^0}{1-\alpha_0^0} + \log(1-\alpha_0^0) + \frac{\alpha_0^0(2-\alpha_0^0)}{(1-\alpha_0^0)^2}\log\alpha_0^0\right]\right\}
\end{aligned} \tag{139}$$

subject to

$$z_1^1 \to 0 \quad \text{as} \quad \alpha_0^0 \to 1, \quad z_1^1 \sim \alpha_s^1\frac{\hat{b}\,Le}{l}\left(\frac{1-\hat{r}}{r\Lambda_0^0}\log\alpha_0^0 + h_1^0\right) \text{ as } \quad \alpha_0^0 \to 0. \tag{140}$$

Homogeneous solutions of (139) are $(1-\alpha_0^0)$ and $(1-\alpha_0^0)^{-1}$. Using the latter, we may seek a particular solution in the form $z_1^1 = (1-\alpha_0^0)^{-1}u$. This leads to a first-order equation for $v \equiv \mathrm{d}u/\mathrm{d}\alpha_0^0$, which, after multiplication by the appropriate integrating factor, may be integrated to obtain an expression for v. A second integration then determines u, and hence z_1^1. Proceeding in this fashion, we construct the general solution for z_1^1 as

$$\begin{aligned}
z_1^1 \;=\; &(1-\alpha_0^0)^{-1}\int_0^{\alpha_0^0}(1-\hat{\alpha})\left[\int_0^{\hat{\alpha}}\frac{\mathrm{RHS}_{139}(\alpha)}{\alpha(1-\alpha)}\,\mathrm{d}\alpha\right]\mathrm{d}\hat{\alpha} \\
&+D_1(1-\alpha_0^0) + D_2(1-\alpha_0^0)^{-1},
\end{aligned} \tag{141}$$

where 'RHS_{139}' denotes the right-hand side of (139) and D_1 and D_2 are constants of integration that lead to terms proportional to the homogeneous solutions. It is readily verified by detailed

examination of the integrand in (141) near $\alpha = 0$ and $\alpha = 1$ that the only singularity in the general solution is that associated with the homogeneous solution $(1-\alpha_0^0)^{-1}$. Consequently, the first matching condition in (140) requires the choice

$$D_2 = -(1-\alpha_0^0)^{-1}\int_0^1 (1-\hat{\alpha})\left[\int_0^{\hat{\alpha}} \alpha^{-1}(1-\alpha)^{-1}\,\mathrm{RHS}_{139}(\alpha)\mathrm{d}\alpha\right]\mathrm{d}\hat{\alpha},$$

so that the family of solutions that vanish as $\alpha_0^0 \to 1$ is given by

$$z_1^1 = -(1-\alpha_0^0)^{-1}\int_{\alpha_0^0}^1 (1-\hat{\alpha})\left[\int_0^{\hat{\alpha}} \frac{\mathrm{RHS}_{139}(\alpha)}{\alpha(1-\alpha)}\,\mathrm{d}\alpha\right]\mathrm{d}\hat{\alpha} + D_1(1-\alpha_0^0). \tag{142}$$

The second matching condition in (140), on the other hand, can only be satisfied if $\hat{r} = 1$ (or, more precisely, $\hat{r} = 1 + \hat{r}^1\epsilon$), since the general solution (141) exhibits no logarithmic behavior as α_0^0 approaches zero. In that case, evaluating (142) at $\alpha_0^0 = 0$, we determine the constant D_1 in terms of h_1^0 as

$$D_1 = h_1^0 + \int_0^1 (1-\hat{\alpha})\left[\int_0^{\hat{\alpha}} \alpha^{-1}(1-\alpha)^{-1}\,\mathrm{RHS}_{139}(\alpha)\,\mathrm{d}\alpha\right]\mathrm{d}\hat{\alpha},$$

and the solution for z_1^1 is thus given by

$$\begin{aligned} z_1^1 \;=\; & -(1-\alpha_0^0)^{-1}\int_{\alpha_0^0}^1 (1-\hat{\alpha})\left[\int_0^{\hat{\alpha}} \frac{\mathrm{RHS}_{139}(\alpha)}{\alpha(1-\alpha)}\,\mathrm{d}\alpha\right]\mathrm{d}\hat{\alpha} \\ & +(1-\alpha_0^0)\left\{\alpha_s^1\frac{\hat{b}\,Le}{l}h_1^0 + \int_0^1 (1-\hat{\alpha})\left[\int_0^{\hat{\alpha}} \frac{\mathrm{RHS}_{139}(\alpha)}{\alpha(1-\alpha)}\,\mathrm{d}\alpha\right]\mathrm{d}\hat{\alpha}\right\}, \end{aligned} \tag{143}$$

where the eigenvalue h_1^0 appears to be undetermined, at least to this order in the analysis. This apparent indeterminacy is resolved at the next order with respect to ϵ, where, in constructing the solution for $z_1^2 \equiv \alpha_0^0 y_1^2$, we require that $h_1^0 = 0$ in order to satisfy the matching conditions at that order. Alternatively, the same conclusion may be reached when one considers that, for nonzero porosities, the inner solution for the original mass-fraction variable Y must ultimately be matched to the outer solution (63). Thus, if $h_1^0 \neq 0$, then (143) implies that the original mass-fraction variable $y_1^1 \sim \alpha_s^1 l^{-1}\hat{b}\,Le\,h_1^0(\alpha_0^0)^{-1}$ as $\alpha_0^0 \to 0$, where $(\alpha_0^0)^{-1} \sim \exp(-r\Lambda_0^0\eta)$ as the inner variable $\eta \to -\infty$. Since this would introduce exponential growth into the inner solution for Y, whereas the outer solution (63), when expanded about $\xi = \xi_r^-$ and written in terms of η, indicates that only algebraic growth of the inner solution with respect to η is compatible with asymptotic matching of the latter to the outer solution. Consequently, we conclude that $h_1^0 = 0$ in the parameter regime analyzed here. We remark that the same argument could have been applied directly to the matching condition (121) to infer the above restriction on the value of $\hat{r}$.

We conclude this section by noting that the required restriction of $\hat{r}$ to values that are relatively close to unity, which corresponds to the assumption of high upstream gas-phase densities, or pressures, has an obvious physical interpretation. In particular, the limit (97) of approximately equal consumption rates for the condensed and gas-phase reaction for relatively small gas-phase heat release is a distinguished limit for the merged-flame regime. That is,

according to the expression for the gas-phase velocity given by (56), it limits the two-phase-flow effect (*i.e.*, the rate of gas-phase convective transport relative to the condensed phase) in the preheat and reaction zones to that associated with thermal expansion of the gas. Larger rates of gas-phase transport with respect to that in the condensed phase would cause the gas-phase reaction to occur increasingly downstream of the condensed reaction, leading to a breakdown in the merged flame structure analyzed here. It is anticipated that larger gas-phase consumption rates would allow for larger gas-phase convective transport arising from smaller upstream gas densities in the merged flame regime, but it would appear that the existence of a merged-flame solution is highly sensitive to pressure (which determines $\hat{r}$ through the gas-phase equation of state) and the relative rates of reaction associated with the condensed and gas-phase portions of the deflagration. These and other conclusions are supported by direct numerical solutions of the reaction-zone problem given by (79)–(83) ([19]).

7. Discussion of the burning rate and conclusions

The dimensional propagation speed $\tilde{U}$, from the definition of Λ_l given in Equation (27), is, from (73) and (87), obtained as

$$\begin{aligned}\tilde{U}^2 \;\sim\; & \frac{\tilde{\lambda}_s \tilde{A}_l}{\tilde{\rho}_s \tilde{c}_s}\beta^0\left[1+\epsilon\frac{T_b^1(2-T_b^0)}{T_b^0(T_b^0-1)}+\cdots\right] \\ & \times(\Lambda_0^0+\epsilon\Lambda_0^1+\cdots)^{-1}\exp\left[-N_l^0\left(1-\epsilon\frac{T_b^1}{T_b^0}+\cdots\right)\right] \\ \sim\; & \frac{\tilde{\lambda}_s \tilde{A}_l}{\tilde{\rho}_s \tilde{c}_s}\cdot\frac{\beta^0}{\Lambda_0^0}e^{-N_l^0}e^{\epsilon\beta^0 T_b^1/(T_b^0-1)+\cdots}\left\{1+\epsilon\left[\frac{T_b^1(2-T_b^0)}{T_b^0(T_b^0-1)}-\frac{\Lambda_0^1}{\Lambda_0^0}\right]+\cdots\right\}, \end{aligned} \tag{144}$$

where T_b, which appears in the definitions of the nondimensional activation energy N_l and the Zel'dovich number β, has been expanded according to (103), and we have introduced the ϵ-independent definitions $N_l^0 \equiv \tilde{E}_l/\tilde{R}^0\tilde{T}_b^0$ and $\beta^0 \equiv (T_b^0-1)N_l^0/T_b^0$. Substituting the expressions (93b) and (134) for Λ_0^0 and Λ_0^1, respectively, and setting ϵ equal to its definition Q_g, we obtain the asymptotic expression for the burning rate, in the specific merged-flame parameter regime considered here, as

$$\begin{aligned}\tilde{U}^2 \;\sim\; & \frac{\tilde{\lambda}_s \tilde{A}_l}{\tilde{\rho}_s \tilde{c}_s}\cdot\frac{rl(T_b^0-1)}{bT_b^0-1-\gamma_s}\beta^0 e^{-N_l^0}e^{\{Q_g\beta^0[\hat{b}^{-1}(T_b^0-1)^{-1}-\alpha_s^1]+\cdots\}} \\ & \times\left\{1+Q_g\left[\frac{2-T_b^0}{\hat{b}T_b^0(T_b^0-1)}-\frac{\alpha_s^1(2-T_b^0)}{T_b^0}+\frac{\hat{l}^1}{2l}-\frac{\pi^2-6}{6(bT_b^0-1-\gamma_s)}\right.\right. \\ & \left.\left.-\frac{(T_b^0-1)}{bT_b^0-1-\gamma_s}\left(\alpha_s^1(\hat{b}-b)+\frac{1+\gamma_s-b}{\hat{b}(T_b^0-1)^2}\right)\right]+\cdots\right\}, \end{aligned} \tag{145}$$

where we have used the expression for T_b^1 given in (103). The first effects of heat release associated with the second step of the reaction model (1) are therefore obtained by studying the terms proportional to Q_g in (145).

The dominant effects associated with gas-phase heat release are contained in the exponential factor whose argument is proportional to $Q_g\beta^0$, which, since $\beta^{-1} \ll Q_g \ll 1$ in our analysis,

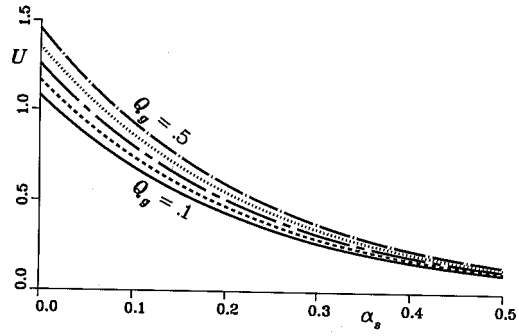

Figure 4. Approximate nondimensional propagation speed $U = \tilde{U}(Q_g, \alpha_s)/\tilde{U}(0,0)$ as a function of $\alpha_s = \alpha_s^1 Q_g$ for $Q_g = 0{\cdot}1$ (solid), $0{\cdot}2$ (dash), $0{\cdot}3$ (chain-dash), $0{\cdot}4$ (dot) and $0{\cdot}5$ (chain-dot), where the remaining parameter values were taken to be the same as those used in the previous figures.

is an exponentially large factor unless $\alpha_s^1 = \alpha_s/Q_g \approx \hat{b}^{-1}(T_b^0 - 1)^{-1}$. Values of the porosity less (greater) than this critical value thus produce a significant increase (decrease) in the burning rate over that of a nonporous material governed solely by the condensed reaction, corresponding to whether or not the perturbation $Q_g T_b^1$ in the burned temperature, which arises from nonzero porosity and the additional heat release associated with the gas-phase reaction, is positive or negative. Since Q_g is positive, the additional heat release associated with the gas-phase reaction enhances the burning rate, but decreasing amounts of solid material that correspond to increasing porosities result in lower overall heat release associated with the condensed-phase reaction, resulting in a critical value of porosity for which these counteracting effects balance. Plots of the nondimensional propagation speed $U = \tilde{U}(Q_g, \alpha_s)/\tilde{U}(0,0)$ as a function of Q_g and α_s are exhibited in Figure 4.

Although the dominant effect associated with nonzero porosity and a second gas-phase reaction step is thus thermodynamic in nature, additional effects are revealed by those terms arising from the correction $Q_g \Lambda_0^1$ to the leading-order burning-rate eigenvalue Λ_0^0, which give rise to the last three terms within the curly brackets in (145). In particular, it is readily seen that a value of the gas-phase thermal conductivity greater (less) than that of the liquid phase tends to increase (decrease) the propagation speed, since larger values of $\hat{l}^1 = (\hat{l} - l)/Q_g$ allow for greater heat transport from the reaction zone back to the preheat region, providing a type of 'excess enthalpy' effect for the condensed phase portion of the reaction, which, in our analysis, is responsible for most of the heat release. The non-thermodynamic effect of nonzero porosity, as reflected by its scaled value α_s^1, has either a negative or a positive effect on the burning rate, depending on whether the difference in heat capacities $\hat{b} - b$ between the gas and the melted material is positive or negative. Assuming the latter, which is the more typical case, we are thus led to the conclusion that, thermodynamic effects aside, slightly porous materials support a faster deflagration speed than their nonporous counterparts, partially overcoming the opposite trend associated with lower burned temperatures described above.

In conclusion, the present analysis has sought to describe some of the effects associated with the deflagration of porous energetic materials arising from two-phase-flow in the presence of a multiphase sequential reaction mechanism. In contrast to previous work for the nonporous case in which the condensed and gas-phase reactions were spatially separated [5], a merged-flame parameter regime, in which both reactions are operative and proceed to completion in a single thin reaction zone, was considered in the present study of a porous material. Following the

formulation of the general reaction-zone problem, it was ultimately determined that additional parameter constraints are required to support this type of structure. In particular, it was deduced that the relative rates of consumption of the condensed and intermediate gaseous species imply a corresponding restriction on the relative rates of convective transport in each phase in order for a single merged flame structure to be maintained. The latter is controlled, at least in part, by the pressure through the gas-phase equation of state. Thus, it was concluded that, when the consumption rates associated with each reaction are approximately equal and most of the heat release occurs in the first reaction step, the merged-flame structure corresponds to a high-pressure regime in which the relative flow of gas with respect to the condensed material arises primarily from thermal expansion of the gas in the preheat and reaction zones. This result is consistent with typical experiments involving HMX and RDX that show the tendency of the primary gas flame to move closer to the propellant surface as the pressure increases. Further parametric studies are in progress and will be reported in future publications.

Acknowledgements

This work was supported by the U.S. Department of Energy under Contract DE-AC04-94AL85000 and by a Memorandum of Understanding between the Office of Munitions (Department of Defense) and the Department of Energy. The author would like to thank Forman Williams for fruitful discussions during the course of this study.

References

1. M. R. Baer and J. W. Nunziato, A two-phase mixture theory for the deflagration-to-detonation transition (DDT) in reactive granular materials. *Int. J. Multiphase Flow* 12 (1986) 861–889.
2. E. I. Maksimov and A. G. Merzhanov, Theory of combustion of condensed substances. *Combustion, Explosion, and Shock Waves* 2 (1966) 25–31.
3. A. G. Merzhanov, The theory of stable homogenous combustion of condensed substances. *Combust. Flame* 13 (1969) 143–156.
4. S. B. Margolis, F. A. Williams and R. C. Armstrong, Influences of two-phase flow in the deflagration of homogeneous solids. *Combust. Flame* 67 (1987) 249–258.
5. S. C. Li., F. A. Williams and S. B. Margolis, Effects of two-phase flow in a model for nitramine deflagration. *Combust. Flame* 80 (1990) 329–349.
6. S. B. Margolis and F. A. Williams, Stability of homogeneous-solid deflagration with two-phase flow in the reaction zone. *Combust. Flame* 79 (1990) 199–213.
7. S. B. Margolis and F. A. Williams, Effects of two-phase flow on the deflagration of porous energetic materials. *J. Propulsion Power* 11 (1995) 759–768.
8. S. B. Margolis and F. A. Williams, Influence of porosity and two-phase flow on diffusional/thermal instability of a deflagrating energetic material. *Combust. Sci. Technol.* 106 (1995) 41–68.
9. S. B. Margolis and F. A. Williams, Effect of gas-phase thermal expansion on stability of deflagrations in porous energetic materials. *Int. J. Multiphase Flow* 22 (1996) 69–91.
10. T. L. Boggs, The thermal behavior of cyclorimethylenetrinitramine (RDX) and cyclotetramethylenetetranitramine (HMX). In: K. K. Kuo and M. Summerfield (eds.), *Fundamentals of Solid-Propellant Combustion*. AIAA *Progress in Astronautics and Aeronautics* 90 (1984) 121–175.
11. S. C. Li and F. A. Williams, Nitramine deflagration: a reduced chemical mechanism for the primary flame facilitating simplified asymptotic analysis. *J. Propulsion and Power* 12 (1996) 302–309.
12. S. B. Margolis and B. J. Matkowsky, Flame propagation with a sequential reaction mechanism. *SIAM J. Appl. Math.* 42 (1982) 1175–1188.
13. S. B. Margolis and B.J. Matkowsky, Steady and pulsating modes of sequential flame propagation. *Combust. Sci. Technol.* 27 (1982) 193–213.
14. J. Peláez and A. Liñán, Structure and stability of flames with two sequential reactions. *SIAM J. Appl. Math.* 45 (1985) 503–522.
15. M. L. Booty, J. B. Holt and B. J. Matkowsky, Condensed phase combustion with a merged sequential reaction mechanism. *Q. J. Mech. Appl. Math.* 43 (1990) 224–249.

16. A. P. Aldushin and K. I. Zeinenko, Combustion of pyrotechnic mixtures with heat transfer from gaseous reaction products. *Combustion, Explosion, and Shock Waves* 27 (1991) 700–703.
17. J. Peláez, Stability of premixed flames with two thin reaction layers. *SIAM J. Appl. Math.* 47 (1987) 781–799.
18. L. Lewin, *Polylogarithms and Associated Functions.* Elsevier North Holland (1981) 359pp.
19. N. Ilincic and S. B. Margolis, Eigenvalue analysis and calculations for the deflagration of porous energetic materials in the merged-flame regime. To appear (1997).